SEEPAGE AND STABILITY ANALYSIS OF GEOSYNTHETIC REINFORED SOIL WALL UNDER RAINFALL

A Dissertation Submitted
in Partial Fulfillment of the Requirement for the Award of the Degree of

MASTER OF TECHNOLOGY
IN
GEOTECHNICAL ENGINEERING
BY

Vasu Yadav
(2K23/GTE/06)

Under the supervision of

Prof. Amit Kumar Shrivastava
Co-Supervisor
Prof. K.S. Rao

DEPARTMENT OF CIVIL ENGINEERING
DELHI TECHNOLOGICAL UNIVERSITY
Main Bawana Road, Delhi-110042, India

May, 2025

DELHI TECHNOLOGICAL UNIVERSITY

(Formerly Delhi College of Engineering)
Shahbad Daulatpur, Main Bawana Road, Delhi-42

CANDIDATE'S DECLARATION

I**, Vasu Yadav (2K23/GTE/06)** student of M. Tech., Geotechnical Engineering, hereby certify that the project dissertation titled **"Seepage and Stability Analysis of Geosynthetic Reinforced Soil Wall under rainfall"** in partial fulfillment of the requirements for the award of the Degree of **Master of Technology (Geotechnical Engineering)**, submitted in the Department of Civil Engineering, Delhi Technological University is an authentic record of my own work carried out during the period from January 2025 to May 2025 under the supervision of **Prof. A.K. Shrivastava** and **Co-Supervisor Prof. K.S. Rao.**

The content presented in the report has not been submitted for the award of any other degree of this or any other institute.

(VASU YADAV)

This is to certify that the student has incorporated all the corrections suggested by the examiners in the thesis and that the statement made by the candidate is correct to the best of our knowledge.

Prof. AMIT KUMAR SHRIVASTAVA
(Supervisor)

Place: Delhi
Date: (Signature of Examiner)

DELHI TECHNOLOGICAL UNIVERSITY

(Formerly Delhi College of Engineering)
Shahbad Daulatpur, Main Bawana Road, Delhi-42

CERTIFICATE BY THE SUPERVISOR(s)

It is certified that **Vasu Yadav (**2K23/GTE/06) has carried out their research work presented in this report entitled "**Seepage and Stability Analysis of Geosynthetic Reinforced Soil Wall under rainfall"** for the award of **Master of Technology** from Department of Civil Engineering, Delhi Technological University, Delhi, under my supervision. The report embodies results of original work, and studies are carried out by the student herself and the contents of the report do not form the basis for the award of any other degree to the candidate or to anybody else from this or any other University/Institution.

Place: Delhi
Date: 31/05/2025

Prof. AMIT KUMAR SHRIVASTAVA
SUPERVISOR & PROFESSOR
Department of Civil Engineering
Delhi Technological University,
Delhi-110042

ABSTRACT

Rainfall-induced seepage and slope instability pose serious challenges to the durability and safety of highway retaining structures, particularly along rainfall-sensitive corridors such as NH-148B (Bhiwani to Hansi). This study investigates the hydraulic behavior and stability of a 10 m high geosynthetic-reinforced soil wall (GRSW) under moderate (15 mm/hr), heavy (30 mm/hr), and very heavy (45 mm/hr) rainfall through 1:30 scale experimental modeling and numerical simulations using SEEP/W and SLOPE/W over a 24-hour period. Pore water pressure (PWP) and volumetric water content (VWC) were monitored at multiple depths, revealing that unreinforced walls exhibited significantly higher water retention and pressure buildup. Geogrid reinforcement reduced PWP and VWC moderately, while geocomposite reinforcement achieved up to 20% lower PWP and 15–25% reduction in VWC compared to unreinforced conditions. Numerical results corroborated the experimental findings, showing that geocomposites maintained lower saturation and more stable suction profiles across rainfall intensities. Stability analysis showed that unreinforced walls failed to meet the IS 6403:1981 minimum factor of safety (FOS) of 1.3, achieving only 1.06 under moderate rainfall. Geogrid reinforcement improved FOS by nearly 30% but fell below safe limits under severe conditions. Geocomposite reinforcement maintained FOS above 1.3 up to heavy rainfall, and after design optimization, offered an overall improvement of approximately 26% in FOS under very heavy rainfall.These findings highlight the superior performance of geocomposites over geogrids and unreinforced systems, due to their combined drainage and reinforcement capabilities, making them a highly effective solution for enhancing the safety and resilience of reinforced soil walls in rainfall-prone environments.

ACKNOWLEDGEMENT

It is with great appreciation that I thank all those who were involved with the work presented in this report.

My first thanks go to my supervisor, **Prof. Amit Kumar Shrivastava**, for his support and critical appraisal which helped me in completing my research work. Their expertise helped in the growth of this work, and their support was unwavering.

I am extremely grateful to **Dr. K. C. Tiwari**, Professor and Head of the Department of Civil Engineering, for the encouragement and support provided during the project work.

I sincerely thank the coordinator, **Dr. Ashok Kumar Gupta**, Professor, for his valuable suggestions for improvement during project reviews.

Also, I would like to extend my gratitude to **Prof. K.S. Rao** for assisting with the collection of data and experiments and analysis that aided me to effectively complete this research. I sincerely thank him for allowing me to carry out the soil experiments in the **KSR GTRS Lab**, which greatly contributed to the practical component of my study.

At the same time, I thank Delhi Technological University for giving me the chance to get the materials and facilities which were needed for the project. I am also grateful to **Gawar Construction Limited and A&T Engineering Pvt. Ltd.** for providing the site location, relevant drawings, and essential materials required for the research.

Last but not least, I send my familiarization to the family for all the overriding affection, care, and patience as well as their strength. Their expectations for me have been useful most of the time and at critical periods of this journey.

VASU YADAV

Roll No. 2K23/GTE/03

Department Of Civil Engineering

Delhi Technological University

Table of Contents

LIST OF TABLES

LIST OF FIGURES

SYMBOLS AND ABBRIVATIONS

q_u	Ultimate bearing capacity (kPa)
c'	Effective Cohesion of the foundation soil (kPa)
γ	Unit Weight of thr Foundation soil (kN/m³)
T_d	Design tensile load in the reinforcement
RF_{total}	Combined reduction factor
τ	Shear strength (kPa)
u	Pore water pressure (kPa)
i	Hydraulic gradient
Cc	Coefficient of curvature
Cu	Coefficient of uniformity
F S	Factor of safety
VWC	Volumetric water content
HCF	Hydraulic Conductivity Function

CHAPTER 1

INTRODUCTION

1.1 GENERAL

In recent decades, India has experienced rapid expansion in road and transport infrastructure, with national highways playing a key role in enhancing connectivity and economic growth. National Highway NH-148B, connecting Bhiwani to Hansi in Haryana, is a vital corridor linking agricultural and industrial regions. To support such development, Geosynthetic Reinforced Soil Walls (GRSWs) have been widely adopted for their cost-effectiveness, structural efficiency, and adaptability to local conditions.

GRSWs, also known as Mechanically Stabilized Earth (MSE) walls, are constructed with compacted soil layers reinforced by geosynthetics—such as geogrids or geotextiles—and faced with concrete panels or wrapped geotextile. These structures offer advantages over traditional retaining walls, including faster construction, flexibility, and better performance under seismic and settlement conditions.

However, GRSWs are vulnerable to rainfall-induced issues. Heavy or prolonged rainfall can increase pore water pressure, reduce matric suction, and weaken soil strength, compromising wall stability. Such conditions are particularly relevant in Haryana, where intense and unpredictable monsoon events are common. Failures often stem from insufficient consideration of hydrological impacts during design, especially in areas with poor drainage.

This study investigates the impact of rainfall on the seepage and stability of GRSWs along NH-148B using numerical tools like SEEP/W and SLOPE/W. The objective is to simulate real-world rainfall conditions and assess the hydro-mechanical behavior of geosynthetic-reinforced systems. The findings aim to improve design practices, optimize drainage provisions, and enhance the durability and safety of highway infrastructure.

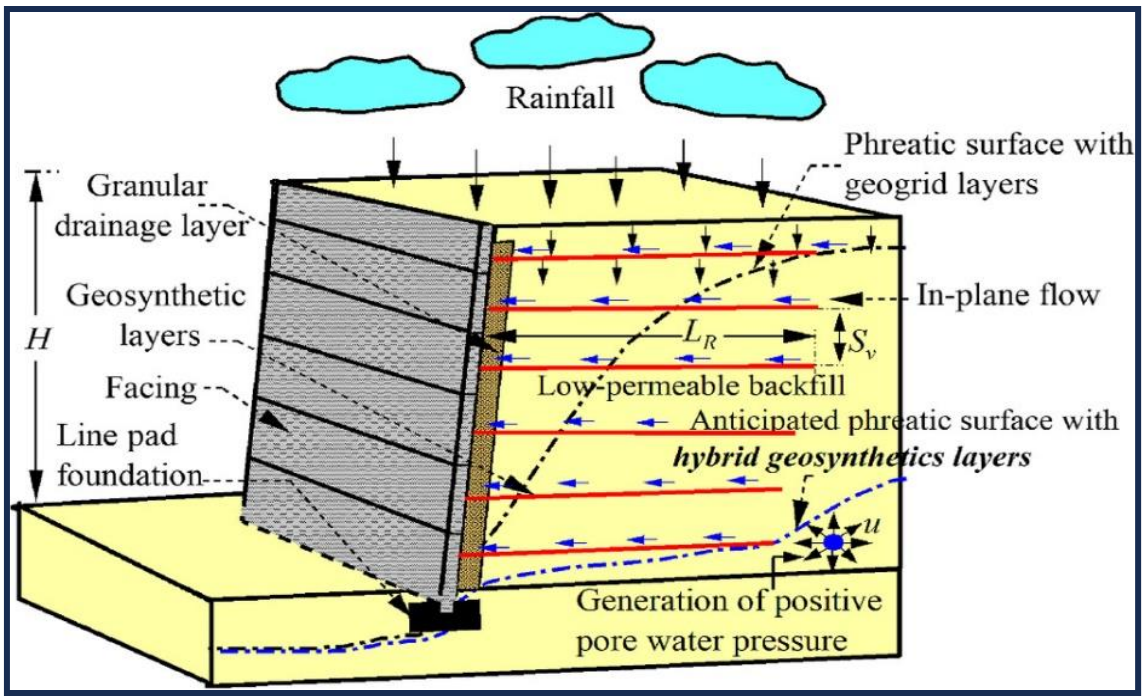

Figure 1.1 Geosynthetic Reinforced Soil Wall under Rainfall (after Midhula Jayanandan et al., 2024)

1.2 CAUSES AND MECHANISMS OF FAILURE IN REINFORCED EARTH WALLS

Reinforced Earth Walls (REWs), particularly those incorporating geosynthetics, have become indispensable in the development of modern infrastructure projects due to their flexibility, cost-efficiency, and ease of construction. These systems are especially prevalent in highway projects such as the NH-148B corridor (Bhiwani to Hansi), where the ability to retain soil economically and sustainably is critical. Despite their advantages, REWs remain susceptible to failure under certain geotechnical, hydraulic, and structural conditions. Failures may arise due to improper design, substandard construction practices, poor drainage, or external environmental influences, notably intense or prolonged rainfall. This section discusses the primary mechanisms and causes of failure in REWs, with emphasis on external, internal, compound, and rainfall-induced failures.

1.2.1 EXTERNAL FAILURE MECHANISMS

External failures compromise the stability of the entire reinforced soil mass. These failures typically include sliding, overturning, and bearing capacity failure.

Sliding Failure occurs when the lateral earth pressures acting on the wall exceed the resisting frictional force at the base. This failure is evaluated using the factor of safety:

$$F\,S_{sliding} = \frac{W\,.\tan(\delta) + c\,.\,A}{p_h} \quad (1)$$

Where:

- W = Weight of the reinforced soil mass (kN)
- δ = Base friction angle (degrees)
- c= Cohesion at the base (kPa)
- A = Area of the base (m²)
- P_H = Horizontal driving force due to earth pressure and surcharge (kN)

If $F\,S_{sliding} < 1.5F\,S$, the structure is deemed unstable under static conditions.

$F\,S_{sliding} < 1.3F\,S$, the structure is deemed unstable under seepage conditions.

$F\,S_{sliding} < 1.1F\,S$, the structure is deemed unstable under seismic conditions.

Overturning Failure arises when the overturning moment caused by lateral loads surpasses the stabilizing moment from the wall's self-weight. The safety against overturning is expressed as:

$$F\,S_{overturning} = \frac{M_R}{M_O} \quad (2)$$

Where:

- M_R = Resisting moment (kNm)
- M_O = Overturning moment (kNm)

Overturning is particularly critical in high or slender walls exposed to significant surcharge loads near the crest.

Bearing Capacity Failure occurs when the applied load exceeds the shear strength of the foundation soil. The ultimate bearing capacity for shallow foundations is given by:

$$q_u = c' N_c + \gamma D_f N_q + 0.5 \gamma B N_\gamma \quad (3)$$

Where:

- q_u = Ultimate bearing capacity (kPa)
- c'= Effective cohesion of the foundation soil (kPa)
- γ = Unit weight of the foundation soil (kN/m³)
- D_f = Depth of foundation (m)
- B = Width of foundation base (m)
- N_c, N_q, N_γ= Bearing capacity factors (dependent on soil friction angle)

External failure is significantly influenced by geometry, foundation soil strength, surcharge loading, and base interface conditions.

1.2.2 INTERNAL FAILURE MECHANISMS

Internal failures relate to the structural integrity of the reinforcement elements embedded within the soil mass. The two dominant types are tensile rupture and pullout failure.

Tensile Rupture happens when the developed tensile force in the reinforcement exceeds its reduced allowable tensile capacity:

$$T_d \leq \frac{T_{ult}}{RF_{total}} \quad (4)$$

Where:

- T_d= Design tensile load in the reinforcement (kN/m)
- T_{ult} = Ultimate tensile strength of the geosynthetic (kN/m)
- RF_{total} = Combined reduction factor, including:

$$RF_{total} = RF_{installation} \cdot RF_{creep} \cdot RF_{chemical} \cdot RF_{biological} \quad (5)$$

These reduction factors account for installation damage, long-term creep, chemical degradation, and biological effects.

Pullout Failure occurs when the interface friction between the reinforcement and surrounding soil is inadequate, resulting in the reinforcement sliding out of the reinforced mass. Pullout resistance is given by:

$$R_{pullout} = 2 \, . L_e \, . \sigma_v \, . \tan(\delta_r) \quad (6)$$

Where:

- L_e = Effective embedded length of the reinforcement beyond the potential failure surface (m)
- σ_v = Vertical overburden pressure at reinforcement level (kPa)
- δ_r = Interface friction angle between geosynthetic and soil (degrees)

Pullout is typically critical near the upper zones of the wall due to lower vertical stress levels.

1.2.3 COMPOUND FAILURE MECHANISM

Compound failure involves a combination of internal and external failure mechanisms and typically results in a complex slip surface that passes through both reinforced and unreinforced zones. This mode of failure is often undetected by conventional limit equilibrium approaches and is better analyzed using advanced numerical simulations such as finite element methods (FEM). These tools allow for more accurate stress-strain modeling and can simulate varying soil properties, reinforcement interactions, and pore pressure conditions simultaneously.

1.2.4 RAINFALL-INDUCED FAILURE

Rainfall is a prominent triggering factor for REW failures, especially in unsaturated soil conditions. As rainwater infiltrates the backfill, the matric suction decreases, which leads to a reduction in effective stress:

$$\sigma' = \sigma - u \quad (7)$$

Where:

- σ'= Effective stress (kPa)
- σ = Total stress (kPa)
- u = Pore water pressure (kPa)

The decrease in effective stress leads to reduced shear strength, governed by the Mohr-

Coulomb criterion:

$$\tau = c' + \sigma' . \tan(\varphi') \quad (8)$$

Where:

- τ = Shear strength (kPa)
- c' = Effective cohesion (kPa)
- ϕ'= Effective internal friction angle (degrees)

Additionally, rainfall induces seepage forces, which act in the direction of flow and reduce soil stability. The hydraulic gradient, defined as:

$$i = \frac{h}{L} \quad (9)$$

Where:

- h = Hydraulic head loss (m)
- L = Length of seepage path (m)

can lead to piping or internal erosion if it exceeds the critical gradient i_c. Poor drainage conditions exacerbate these effects, especially in zones with low permeability or inadequate weep holes and drainage layers.

The incorporation of geocomposites and prefabricated vertical drains (PVDs) within the reinforced zone can mitigate the adverse effects of rainfall by enhancing drainage and dissipating excess pore pressures. However, their effectiveness depends on correct design, alignment, and maintenance.

1.3 EFFECT OF RAINFALL ON REINFORCED EARTH WALLS

Rainfall is a critical environmental factor affecting the performance and long-term stability of reinforced earth walls. Infiltration of rainwater into the backfill alters the hydro-mechanical behavior by increasing moisture content and potentially saturating the soil. As infiltration advances, matric suction in unsaturated soils—key to shear strength—reduces, leading to a drop in apparent cohesion. This effect is more significant in fine-grained or poorly draining soils, common along the NH-148B corridor. Rising pore water pressure during heavy rainfall further reduces effective stress, thereby compromising shear strength, as per the Mohr-Coulomb criterion ($\tau = c' + \sigma' \tan(\Phi')$).

Rainfall-induced seepage within the reinforced zone also generates hydraulic forces along the flow path, destabilizing the reinforcement and soil mass. Without adequate drainage—such as weep holes, gravel blankets, or geosynthetic drains—water can accumulate, increasing hydrostatic pressure and the driving forces on the wall. This may lead to localized issues like face bulging, slumping, or overall instability. Additionally, cyclic wetting and drying from seasonal rains can cause volumetric changes in expansive soils and fatigue in geosynthetics, weakening the soil-reinforcement bond. In severe cases, intense rainfall may trigger piping or internal erosion in loose, fine-grained backfill, resulting in sudden and progressive wall failure.

1.4 OVERVIEW OF GEOSTUDIO SOFTWARE

GeoStudio is a widely recognized suite of integrated software tools developed by Geo-Slope International Ltd. for analyzing geotechnical and geo-environmental engineering problems. It includes several powerful modules such as SEEP/W, SLOPE/W, SIGMA/W, and TEMP/W, which allow users to simulate seepage, slope stability, stress-strain behavior, and thermal analysis in soil systems. In the context of reinforced earth walls, SEEP/W is particularly valuable for modeling water flow and pore water pressure changes during rainfall events, while SLOPE/W enables rigorous slope stability analysis under both saturated and unsaturated conditions. The software uses finite element methods to simulate real-world geotechnical problems with high accuracy, allowing for the assessment of complex interactions between soil, water, and reinforcement materials. Its ability to model transient conditions, such as rainfall infiltration and changes in groundwater levels, makes GeoStudio especially relevant for evaluating the stability of geosynthetic-reinforced walls under rainfall-induced seepage. With its user-friendly interface, strong graphical visualization, and interoperability between modules, GeoStudio provides a comprehensive and reliable platform for advanced geotechnical analysis.

1.5 DIFFERENT METHODS OF ANALYSIS

1.5.1 LIMIT EQUILIBRIUM METHOD (LEM)

The Limit Equilibrium Method is a widely used traditional technique to evaluate the stability of reinforced earth walls. It assumes a potential failure surface and analyzes the balance between driving and resisting forces or moments. This method is especially useful for calculating the factor of safety against sliding, overturning, and global stability. Although simple and practical, LEM does not consider stress-strain behavior or time-dependent changes, making it less suitable for modeling complex or transient conditions like rainfall infiltration.

1.5.2 FINITE ELEMENT METHOD (FEM)

The Finite Element Method is an advanced numerical approach that models the stress-strain behavior of soil-reinforcement systems under various loading conditions. It discretizes the wall and surrounding soil into small elements and solves governing equations based on soil mechanics principles. FEM can simulate complex phenomena such as rainfall infiltration, pore water pressure variation, and reinforcement-soil interaction. It is highly accurate and useful for capturing progressive failure and deformation but requires detailed input parameters and computational resources.

1.6 GEOSYNTHETICS (GEOCOMPOSITES)

Geosynthetics are a broad class of polymeric materials used in geotechnical engineering to improve the mechanical and hydraulic behavior of soil systems. They include geotextiles, geogrids, geomembranes, geonets, and geocomposites—each designed for specific applications such as separation, filtration, drainage, reinforcement, and containment. Among these, geocomposites are increasingly favored in the construction of reinforced earth walls due to their ability to integrate multiple functions into a single product. A geocomposite typically consists of a drainage core, such as a geonet or cuspated plastic structure, bonded with one or more geotextile layers to provide filtration and reinforcement. The materials commonly used in manufacturing geocomposites are high-density polyethylene (HDPE), polypropylene (PP), and polyester

(PET) due to their high tensile strength, low creep characteristics, chemical resistance, and long-term durability under both static and dynamic loading conditions (et al., Koerner, 2012).

In the context of reinforced earth walls, geocomposites serve a dual function: they reinforce the soil mass by resisting tensile stresses and simultaneously provide a drainage path to reduce pore water pressure, particularly during and after rainfall events. This makes them particularly suitable for sites like the NH-148B highway stretch from Bhiwani to Hansi, where seasonal monsoon rains can significantly increase the risk of slope failure due to water ingress. The integration of drainage within the reinforcement system prevents the buildup of hydrostatic pressure, which is one of the primary causes of wall distress during prolonged rainfall. According to Bathurst et al. (2011), geosynthetic reinforcements can effectively enhance wall performance and extend service life by improving internal and global stability under varying moisture conditions.

1.7 OBJECTIVES OF THE RESEARCH

The primary objectives of this research are:

- To evaluate the seepage behavior and pore water pressure development in geosynthetic-reinforced soil walls under varying rainfall conditions.
- To analyze the stability of reinforced earth walls using numerical modeling through GeoStudio software.
- To assess the effectiveness of geocomposites in enhancing drainage and stability performance of reinforced soil structures.
- To investigate failure mechanisms and critical conditions influencing wall performance during rainfall infiltration.

CHAPTER 2

LITERATURE REVIEW

Zou et al. (2024) [1] investigated the hydro-mechanical behavior of geogrid-reinforced expansive soil slopes through two-year field monitoring and FLAC2D simulations. The study showed that geogrid inclusion reduced deformation and swelling during rainfall. However, it highlighted the degradation of soil–reinforcement bond due to drying–wetting cycles. The study recommended long-term climatic cycle consideration. This helps improve the durability of reinforced slopes under environmental fluctuations.

Liu et al. (2024) [2] used CFD-DEM simulations to study rainfall-induced failures in sandy soil excavations. Different rainfall patterns caused varying failure mechanisms, including toe sliding and sand boiling. Increased precipitation intensified deformation and expanded the displacement zone. A simplified method was proposed for estimating primary displacement zones. This helps predict failures in erodible sandy excavations during extreme weather.

He et al. (2024) [3] analyzed the deformation of metro tunnels affected by river excavation in soft soils through 3D finite element modeling and field monitoring. Vertical displacements were primarily triggered by excavation above tunnels, while horizontal shifts resulted from adjacent digging. Soil reinforcement using cement slurry and concrete forms proved effective in reducing tunnel deformation. The study validated model accuracy using real-time measurements. Insights help protect tunnel systems in urban excavation zones.10

Guo et al. (2024) [4] developed a 3D numerical model to study pore water pressure variations in vegetated slopes under diverse rainfall patterns. Results showed that root-induced suction enhanced slope stability during short, intense rainfall but had limited

impact during prolonged rainfall. Rainfall type and slope angle were key factors in hydrological response. Transpiration effects persisted even after heavy rain events. The study aids bioengineering applications for slope stabilization.

Chaiprakaikeow et al. (2024) [5] conducted a field study on a geosynthetic-reinforced soil wall with side drainage to evaluate suction, moisture, and stiffness behavior. Seasonal moisture variations were monitored using sensors and SASW tests to assess shear modulus changes. Results indicated stiffness sensitivity to pore-water pressure, especially under positive pressure conditions. Moisture distribution varied with depth, influenced by drainage system placement. The study offers design insights for GRS walls in unsaturated, sloped terrains.

Zhu et al. (2023) [6] analyzed wetting deformation in loess high-fill embankments due to rainfall and groundwater rise. Field data and FEM modeling showed that groundwater uplift induced three times more settlement than rainfall. A strain–time empirical model was developed to predict deformation. Rainfall intensity affected infiltration depth, showing a Y-shaped moisture profile. Recommendations for drainage and reinforcement were proposed.

Li et al. (2023) [7] proposed a thermal-seepage coupled numerical model to simulate artificial ground freezing processes. By integrating measured soil freezing curves, the model achieved better accuracy in predicting freeze wall development under seepage. It highlighted the limitations of traditional heat capacity methods. The new approach offered improvements in robustness and physical representation. Findings contribute to safer underground construction using ground freezing technology.

Guzmán-Martínez et al. (2022) [8] used a coupled infiltration–deformation model to assess capillary barrier effects in reinforced embankments. Results showed that both hydraulic and mechanical properties significantly affect pore pressure development.

Parameters like suction, void ratio, and permeability controlled barrier performance. Capillary barriers reduced infiltration but may cause instability if drainage is poor. The study supports integrating hydro-mechanical factors in geosynthetic designs.

Xu et al. (2022) [9] modeled slope behavior under post-earthquake rainfall using FEM, incorporating crack-induced permeability and stiffness degradation. Earthquake-damaged slopes experienced deeper slip surfaces and higher deformations. The model aligned with centrifuge test results. Findings emphasized including earthquake-induced damage in stability assessments. This is crucial for landslide prevention in seismic regions.6

Xu et al. (2022) [10] investigated seepage failure in a deep foundation pit under confined aquifer conditions. The failure was caused by defects in the waterproof curtain and a weak region around an abandoned pile. A reconstruction strategy using grouting, steel struts, and a deep TRD wall successfully stabilized the site. The incident underscores the importance of waterproofing design and proper dewatering in layered aquifer systems. Lessons learned offer insight into safer deep excavation practices.

Wang et al. (2022) [11] investigated the stability of a steep bank slope and a thin-walled rock cofferdam during excavation for an intake foundation. Numerical simulations revealed that excavation induced deformation and failure in the rock wall. Reinforcement using steel tubular piles effectively prevented collapse. Monitoring confirmed that slope stability was maintained with proper support. The findings guide excavation practices in challenging riverbank terrains.

Nunes et al. (2022) [12] performed a numerical analysis on how different climate conditions affect the performance of geosynthetic-reinforced soil walls. They observed that high rainfall and low evaporation reduced suction, weakening wall stability. Geocomposites showed reduced drainage efficiency under saturated conditions. Climate factors like rainfall intensity and frequency played a crucial role. The study emphasizes

considering environmental factors in GRS wall design.

Vibha and Divya (2021) [13] numerically analyzed the performance of MSE walls with marginal lateritic backfill under rainfall. The study compared standard geogrid-reinforced walls with those using composite geogrids for reinforcement and drainage. Results showed complete suction loss and reduced safety in standard geogrid walls within 2.176 days. Composite geogrids maintained suction and a stable factor of safety throughout rainfall. This highlights the effectiveness of composite geogrids in improving wall stability under wet conditions.

Rahardjo et al. (2020) [14] proposed the GeoBarrier System (GBS) combining reinforced soil and capillary barriers to improve slope stability under rainfall. Field monitoring and numerical analysis showed GBS minimized infiltration and maintained suction in reinforced zones. GBS was found resistant to local failures, with sliding at the base being the critical failure mode. Recycled materials were used, promoting sustainability. The system proved effective under extreme rainfall events.

Bhattacherjee and Viswanadham (2015) [15] conducted numerical simulations to evaluate the stability of hybrid-geosynthetic-reinforced soil slopes under rainfall. The study showed that the inclusion of both geotextiles and geogrids reduced pore water pressure and deformation. Hybrid layers provided combined drainage and reinforcement, enhancing slope performance across varying rainfall intensities. Results indicated improved safety factors compared to unreinforced and singly reinforced slopes. The study supports hybrid geosynthetics as an effective solution for slope stabilization in low-permeability soils under wet conditions.

CHAPTER 3

STUDY LOCATION

3.1 SITE DESCRIPTION

The study location is situated at Chainage 24+200 along National Highway 148B as mentioned figure 3.1, which forms a critical segment of the transportation corridor between Bhiwani and Hansi in the state of Haryana, India. The geographic coordinates of the site are 28°57'08" N latitude and 76°02'56" E longitude, placing it in the vicinity of Bawani Khera Tehsil, a semi-urban area with growing infrastructure and agricultural significance. The exact location and surrounding topography have been identified and verified using Google Earth Pro.

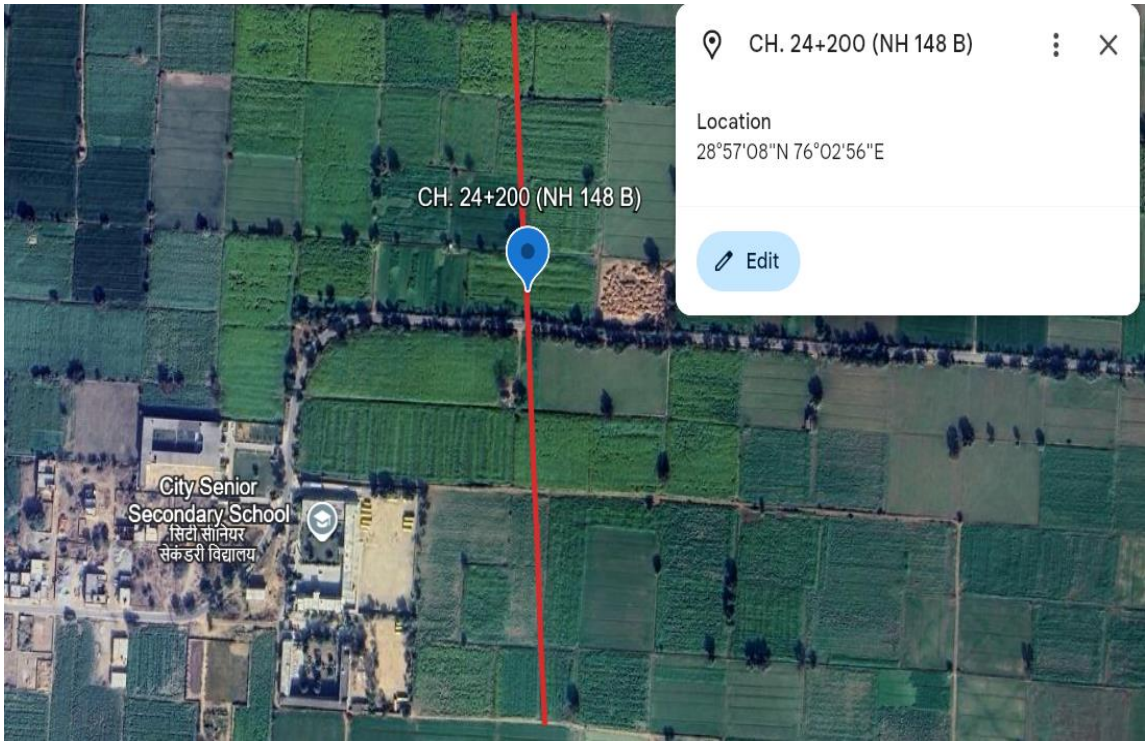

Figure 3.1 Location map of the project site at Chainage 24+200 on NH-148B (Bhiwani–Hansi section), Haryana

Figure 3.2 Reinforced Earth Wall at Chainage 24+200

3.2 TOPOGRAPHY AND DRAINAGE PATTERN

The study area near Bawani Khera in Bhiwani district lies on a predominantly flat and level plain, with occasional sand dunes and minor rocky outcrops, as reported by the Indian Geological Survey. Elevation ranges between 135 to 339 meters above mean sea level, indicating low topographic relief. The region lacks perennial rivers, and the only notable drainage feature is the ephemeral Dohan River, which flows during intense rainfall events. Drainage is poorly developed with low-lying channels, and traces of palaeo-channels suggest historical fluvial activity. These geomorphological features significantly influence surface runoff and subsurface seepage behavior.

3.3 GROUNDWATER CONDITION AT SITE LOCATION

According to the Central Ground Water Board (2012) groundwater level map of Bhiwani district, the variations in pre-monsoon and post-monsoon groundwater depths are illustrated in Figure 3.3 and Figure 3.4, highlighting seasonal fluctuations in the water table across the region.

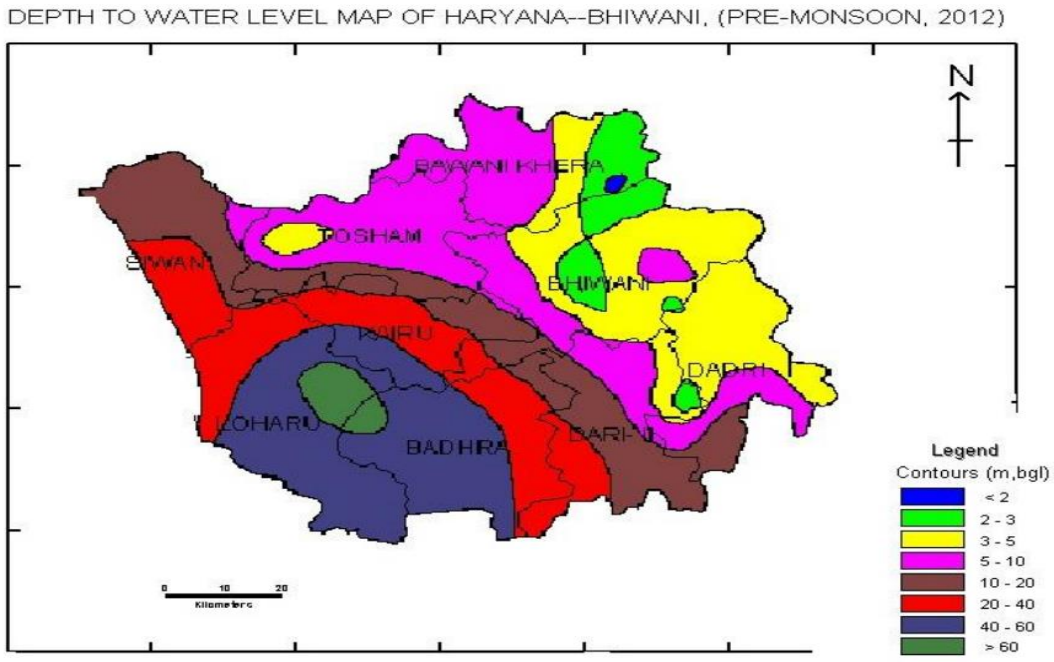

Figure 3.3 Depth of water level of Bhiwani, (Pre-Monsoon)

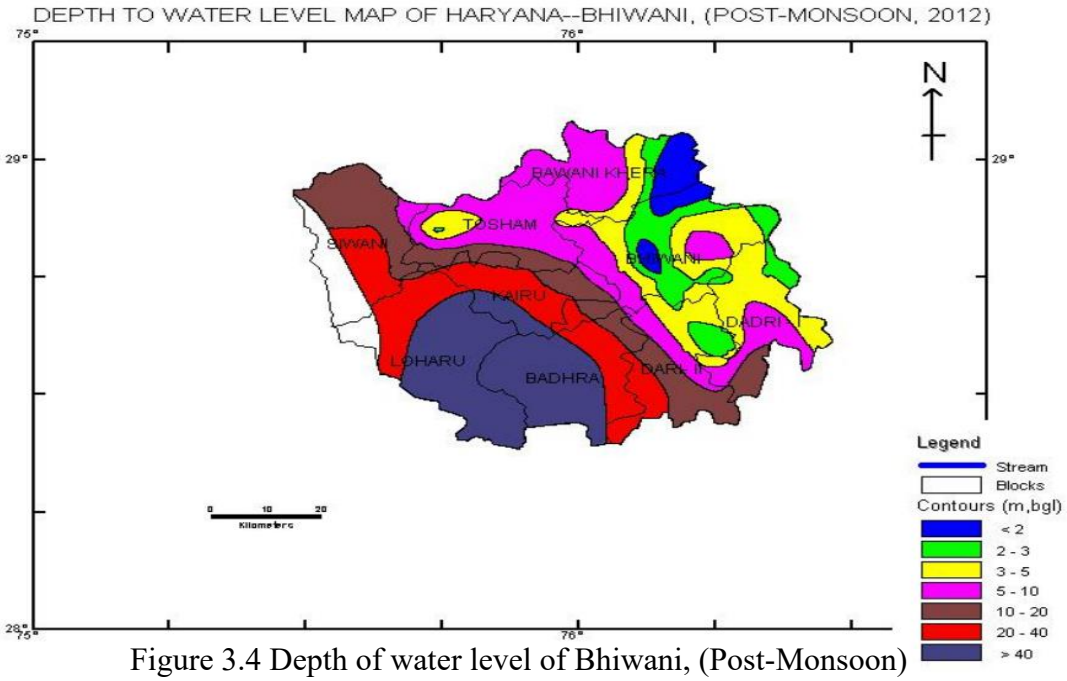

Figure 3.4 Depth of water level of Bhiwani, (Post-Monsoon)

3.4 GEOTECHNICAL PROPERTIES OF SOIL

At Chainage 24+200 on NH-148B (Bhiwani–Hansi section), a subsurface investigation to a depth of 6 meters identified two distinct soil layers. The lower 2.5 meters is composed of silty clay with a unit weight of 20 kN/m³, cohesion of 102.98 kPa, and a low internal friction angle of 4°, indicating weak shear resistance. Above this lies a 3.5-meter silty sand layer with better strength characteristics—19.5 kN/m³ unit weight, 0.9 kPa cohesion, and a friction angle of 27.3°. The reinforced backfill comprises poorly graded sand (SP) up to 10 meters high, having a unit weight of 17.89 kN/m³, minimal cohesion (0.139 kPa), and a high friction angle of 35°, ideal for reinforced structures. The groundwater table, located 2 meters below ground level, influences pore pressures and seepage behavior. These stratigraphic and geotechnical parameters have been integrated into GeoStudio for rainfall-induced seepage and stability modeling.

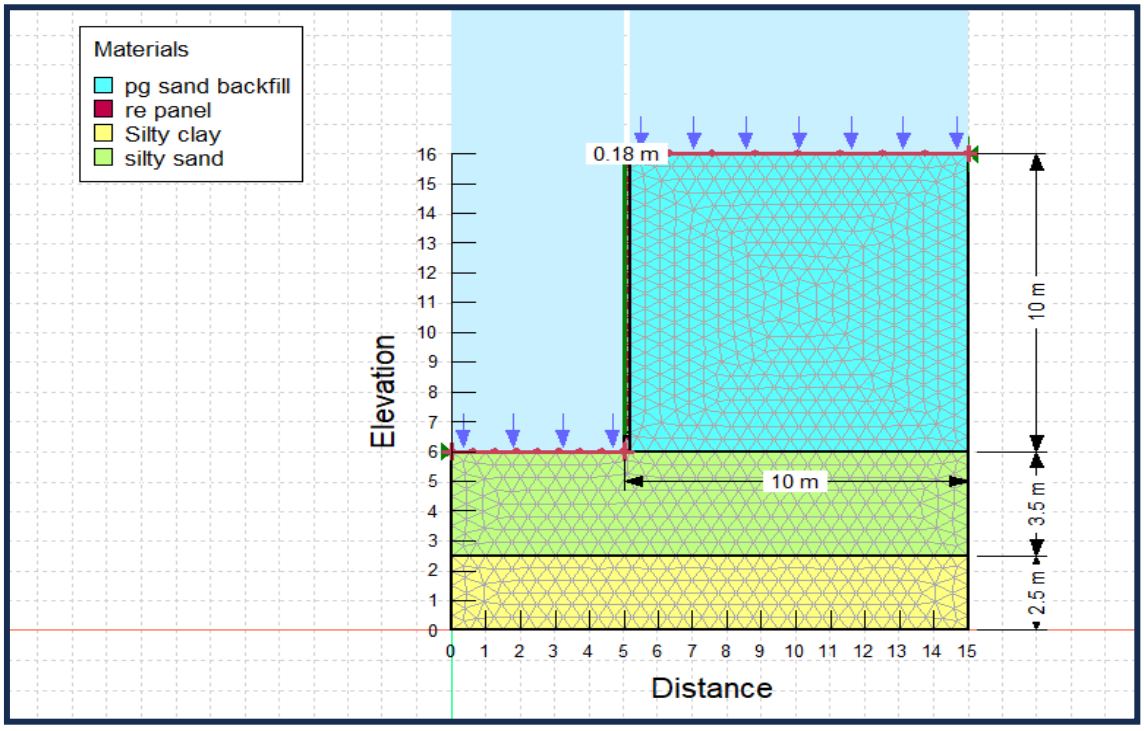

Figure 3.5 Geometry of study of Reinforced Soil Wall without Reinforcement

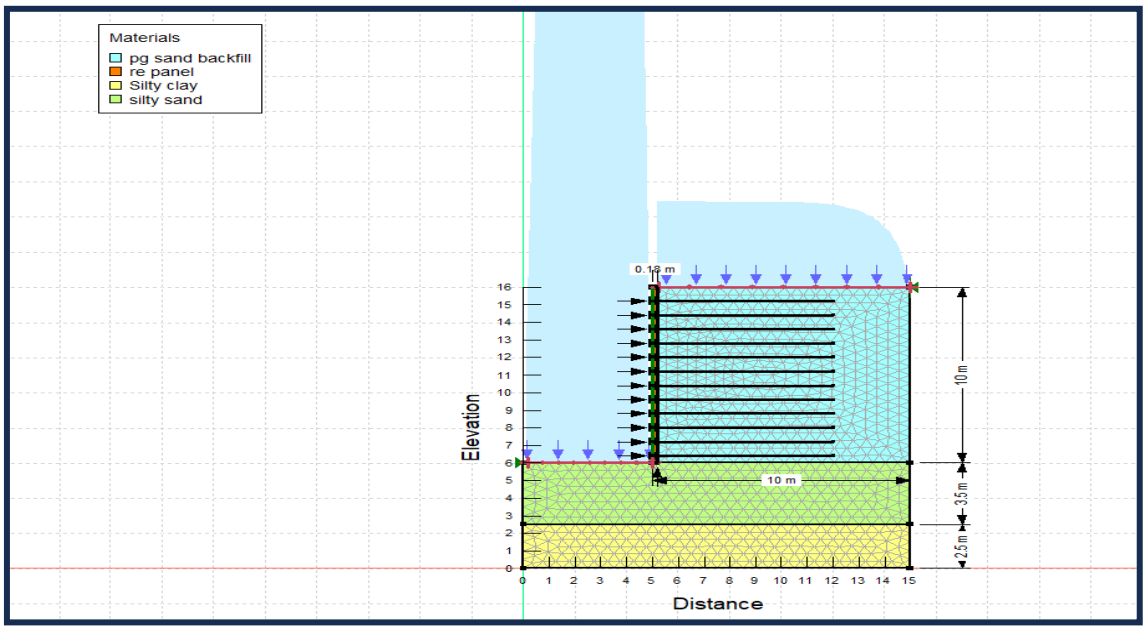

Figure 3.6 Geometry of study of Reinforced Soil Wall with Geo-Synthetic reinforcement (0.7H)

3.3 RAINFALL CHARACTERISTICS

The study area near Bawani Khera in Bhiwani district receives an average annual rainfall of approximately 420 mm, as reported by the Central Ground Water Board (CGWB). The region experiences a distinct monsoonal climate, with the majority of precipitation occurring between late June and late September, driven by the southwest monsoon. Rainfall events are often short-duration but high-intensity, contributing to rapid surface runoff and potential infiltration into the backfill material of reinforced soil structures.

The annual rainfall data for Bhiwani district from the year 2002 to 2011 has been compiled based on records from the Integrated Watershed Management Programme (IWMP, Sixth Edition) and is presented in Table 3.1 and Figure 3.7. Additionally, the monthly rainfall distribution for the year 2021, as reported by the Central Ground Water Board (CGWB), is illustrated in Figure 3.8. These datasets provide valuable insights into both long-term precipitation trends and recent rainfall variability, which are critical for evaluating the hydrological impact on the stability and seepage behavior of geosynthetic-reinforced soil walls at the study location.

Table 3.1 Annual Rainfall Data for Bhiwani, Haryana (2002–2011) (As per IWMP, Sixth Edition)

S.No.	Year	Rainfall (mm)
1	2002	187
2	2003	431
3	2004	567
4	2005	573
5	2006	341
6	2007	413
7	2008	946
8	2009	389
9	2010	969
10	2011	551
Average		**537**

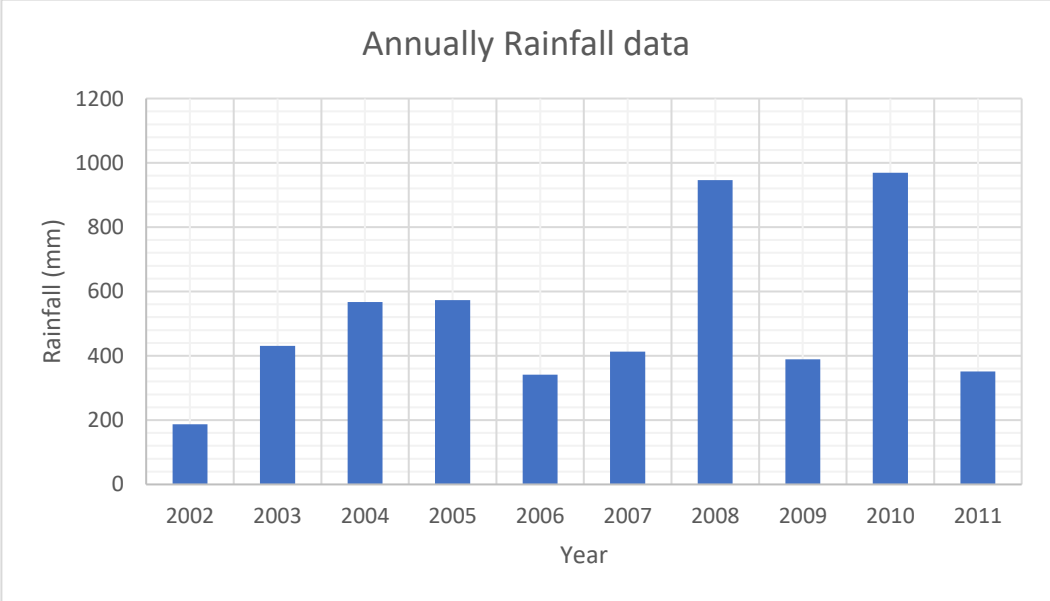

Figure 3.7 Annual Rainfall Data of Bhiwani, Haryana (2002–2011)

Source: IWMP, Sixth Edition

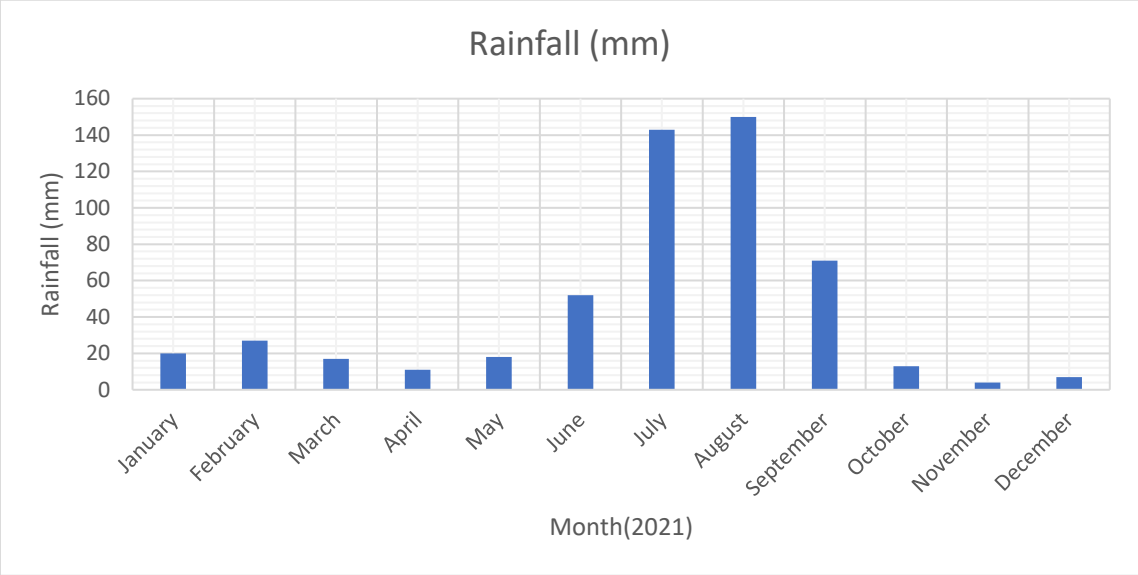

Figure 3.8 Monthly Rainfall Data of Bhiwani, Haryana for the Year 2021*Source: Central Water Ground Board (CWGB)*

CHAPTER 4

METHODOLOGY

This chapter outlines the systematic methodology adopted to analyze the seepage and stability behavior of a geosynthetic reinforced soil (GRS) wall subjected to rainfall. The approach integrates numerical modeling and analytical techniques to achieve accurate and reliable results. The overall workflow followed in this study is illustrated in the flow chart provided below.

Figure 4.1: Workflow Diagram Illustrating the Key Stages of the Study

4.1 EXPERIMENTAL INVESTIGATIONS

A series of laboratory tests were conducted to determine the geotechnical properties of the soil samples collected from the study area. The procedures and methodologies adopted for each test are outlined below, aimed at accurately characterizing the soil behavior relevant to the analysis of reinforced soil structures.

4.1.1 GRAIN SIZE DISTRIBUTION ANALYSIS (IS 2720 (PART 4) – 1985)

Grain size analysis was performed as per **IS 2720 (Part 4) – 1985** using the wet sieve method, suitable for fine-grained soils. A 200 g soil sample was mixed with 1 liter of water containing 2 g of sodium hexametaphosphate as a dispersing agent. After thorough mixing and soaking to promote deflocculation, the suspension was washed through a 75-micron sieve until the wash water ran clear. The retained soil was then oven-dried at 105–110°C for 24 hours.

The dried sample was subjected to mechanical sieve analysis using standard sieves (4.75 mm to 0.075 mm). The percentage passing through each sieve was recorded and used to plot the grain size distribution curve. From this, D10, D30, and D60 values were obtained to calculate the Coefficient of Uniformity (Cu) and Coefficient of Curvature (Cc). These parameters are essential for classifying the soil and assessing its gradation, permeability, compaction characteristics, and suitability for use in reinforced soil structures.

Coefficient of Uniformity (Cu):

$$C_u = \frac{D_{60}}{D_{10}} \tag{10}$$

Where:

- D_{60} = Particle diameter at 60% finer by weight
- D_{10} = Particle diameter at 10% finer by weight

Interpretation:

- For well-graded sand, Cu > 6
- For well-graded gravel, Cu > 4

- If Cu is low, the soil is uniformly graded (i.e., poorly graded)

Coefficient of Curvature (Cc):

$$C_c = \frac{(D_{30})^2}{D_{10}\ X\ D_{60}} \tag{11}$$

Where:

- D_{30} = Particle diameter at 30% finer by weight

Interpretation:

- For a soil to be considered well-graded, $1 \leq Cc \leq 3$
- If Cc falls outside this range, the soil may be poorly graded despite a high Cu.

These criteria are essential for classifying soils based on **USCS (Unified Soil Classification System)**.

Figure 4.2 Standard Set of Sieves Arranged in Descending Order of Size for Grain Size Distribution Analysis

4.1.2 DETERMINATION OF SPECIFIC GRAVITY (IS 2720 (PART 3) – 1980)

The specific gravity (Gs) of the soil was determined using the density bottle method as per **IS 2720 (Part 3) – 1980**, suitable for fine-grained soils passing through a 2 mm sieve. About 7 grams of oven-dried soil was placed into a clean, dry density bottle. Distilled water was then added, and the bottle was placed in a water bath at 27 °C for 6 to 7 hours. This process ensured thermal equilibrium and removal of entrapped air for accurate measurement of specific gravity. The specific gravity was calculated using the following formula:

$$G_S = \frac{(W_2 - W_1)}{(W_4 - W_1) - (W_3 - W_2)} \quad (12)$$

Where:

- W_1= Weight of empty density bottle
- W_2 = Weight of density bottle with dry soil
- W_3 = Weight of density bottle with soil and water
- W_4 = Weight of density bottle filled with water only

This value of specific gravity is a fundamental parameter in geotechnical engineering and is critical for determining the void ratio, porosity, degree of saturation, and unit weight relationships in soil mechanics, which influence the design and analysis of reinforced soil structures.

Figure 4.3 Density Bottle Apparatus Used for Determination of Specific Gravity of Soil

4.1.3 MODIFIED PROCTOR COMPACTION TEST (IS 2720 (PART 8) – 1983)

The Modified Proctor Test was conducted in accordance with **IS 2720 (Part 8) – 1983** to determine the Maximum Dry Density (MDD) and Optimum Moisture Content (OMC) of the soil. These parameters are critical in assessing the compaction characteristics of soil, which directly influence the stability and strength of Geosynthetic Reinforced Soil (GRS) walls, especially under varying field moisture conditions.

In this test, soil passing through a 4.75 mm IS sieve was used, and a sample weight of approximately 2.7 kg was prepared. A 1000 cc mould (commonly referred to as the small compaction mould) was employed along with a 4.89 kg rammer having a drop height of 450 mm. The soil was compacted in five equal layers, each receiving 25 blows to simulate field compaction energy.

The dry density (ρd) for each moisture content was calculated using the formula:

$$\rho_d = \frac{W}{V(1 + \frac{w}{100})} \quad (13)$$

Where:

- W = Weight of compacted soil
- V = Volume of the mould (1000 cc)
- w = Moisture content (%) of the sample

A compaction curve was plotted between moisture content and dry density to determine the Maximum Dry Density (MDD) and Optimum Moisture Content (OMC).

Relevance to Reinforced Earth Wall Construction:

The determined MDD and OMC are essential for achieving proper compaction of the reinforced fill material, which enhances shear strength, reduces settlement, and improves long-term performance of the GRS wall. These values are used in the field during construction to monitor and control the in-situ compaction using field density tests such as the Sand Replacement Method or Nuclear Density Gauge, ensuring the fill material meets the design specifications. Proper compaction as per lab-determined MDD and OMC prevents excessive deformation or failure of the wall under service loads and during rainfall infiltration.

Figure 4.4 Modified Proctor Test Setup for Determination of Maximum Dry Density and Optimum Moisture Content

4.1.4 CONSTANT HEAD PERMEABILITY TEST (IS 2720 (PART 17) – 1986)

The Constant Head Permeability Test was conducted as per the guidelines of **IS 2720 (Part 17) – 1986**, to determine the coefficient of permeability (k) of the soil sample, a critical parameter influencing seepage behavior in Geosynthetic Reinforced Soil (GRS) walls, especially under rainfall conditions.

A 2.5 kg soil specimen, passing through the 4.75 mm IS sieve, was prepared and compacted into a permeameter mold to the desired density. The soil was saturated prior to testing by gradually adding water to achieve the required water content, as obtained from laboratory moisture content determination, ensuring all voids were filled. The test was conducted under a constant hydraulic head to simulate steady-state seepage conditions.

The coefficient of permeability was determined using Darcy's Law:

$$k = \frac{QL}{hAt} \tag{14}$$

Where:

- k = Coefficient of permeability (cm/s)
- Q = Volume of water collected (cm^3)
- L = Length of the soil specimen (cm)
- A = Cross-sectional area of the specimen (cm^2)
- h = Hydraulic head (cm)
- t = Time taken for flow (s)

Figure 4.5 Permeability Apparatus Used for Determination of Coefficient of Permeability

This test is vital for the analysis of seepage and stability in the reinforced soil wall model, as it helps simulate how water infiltrates and migrates through the backfill and foundation layers during rainfall events. The results are directly applied in numerical simulations (e.g., SEEP/W models) to evaluate pore water pressure buildup and its influence on wall performance.

4.1.5 DIRECT SHEAR TEST (IS 2720 (PART 13) – 1986)

The Direct Shear Test was carried out in accordance with **IS 2720 (Part 13) – 1986** to evaluate the shear strength parameters—cohesion (c) and angle of internal friction (ϕ)—of the soil used in the reinforced soil wall system. This test is particularly significant for understanding the behavior of soil under shear stress, which directly impacts the stability of geosynthetic-reinforced structures under both static and seepage conditions.

Three soil specimens, each weighing approximately 182.5 g, were prepared. The weight was calculated using the formula:

$$W = \rho_d V \tag{15}$$

- W = Weight of the soil specimen
- ρ_d = Maximum dry density (from Modified Proctor Test)
- V = Volume of the shear box

Water was added to bring the specimens to their Optimum Moisture Content (OMC), and the soil was then sealed and left to condition for several hours to ensure uniform moisture distribution and partial saturation.

Each specimen was placed into the shear box of the direct shear apparatus and subjected to three different normal stresses:

- σ_1=0.5 kg/cm2
- σ_2=1.0 kg/cm2
- σ_3=1.5 kg/cm2

A strain-controlled loading was applied at a constant rate of 1.25 mm/min, and both horizontal displacement and shear force were recorded throughout the test until failure occurred. The corrected shear area was determined using:

$$A_c = A(1 - \frac{\delta}{60}) \tag{16}$$

Where:

- A_c = Corrected area
- A = Original area of the specimen
- δ_c = Horizontal displacement

The shear stress (τ) at each stage was computed as:

$$\tau = \frac{P}{A_c} \tag{17}$$

Where P is the measured shear force.

By plotting shear stress versus normal stress, the Mohr-Coulomb failure envelope was drawn, from which the cohesion (c) and angle of internal friction (ϕ) were derived.

Application to the Project:

This test provides critical input parameters for the numerical modeling and stability analysis of the Geosynthetic Reinforced Soil Wall under rainfall and seepage conditions. The values of c and ϕ are directly used in limit equilibrium methods and finite element simulations (e.g., SIGMA/W and SLOPE/W) to evaluate sliding resistance, safety factor, and deformation behavior of the reinforced system under different loading and saturation scenarios.

Figure 4.6 Direct Shear Test

4.2 EXPERIMENTAL MODELLING OF REINFORCED EARTH WALL

To study the stability of a geosynthetic-reinforced soil wall under different rainfall intensities, a scaled laboratory model was developed to simulate field conditions at Chainage 24+200 on NH-148B (Bhiwani–Hansi). The prototype wall, measuring 10 m in height, width, and length, was reduced to a 1:30 scale, resulting in a 30 cm cube model. The model used poorly graded sand (SP) matching site conditions, with a maximum dry density of 1.82 g/cc and an OMC of 11%. Soil was compacted in five layers; each 8.2 cm thick layer reduced to 6 cm after compaction using 70 blows per layer from a standard rammer. Three sides of the model (bottom, rear, and one lateral) were fixed to mimic field confinement, while the front remained open for deformation observation.

Rainfall was simulated at 15 mm/hr, 30 mm/hr, and 45 mm/hr, reflecting regional intensities defined by NCHM (National Centre for Hydrology & Meteorology). Base drainage was provided to replicate field-drained conditions. Pore water pressures were calculated using $u = \gamma_w . h$, with γ_w as 9.81 kN/m³. Water content was measured through oven-drying, and wall deformation was tracked using dial gauges at different heights. This setup allowed detailed observation of moisture movement, pore pressure, and deformation under varying hydrological loads.

Figure 4.7 Reinforced Soil Earth Wall Experimental Model under Rainfall

4.3 NUMERICAL MODELLING

To complement the experimental investigation, a comprehensive numerical modeling approach was adopted to simulate the behavior of the geosynthetic-reinforced soil (GRS) wall under varying rainfall intensities. The modeling was performed using the GeoStudio suite, primarily utilizing SEEP/W for seepage analysis and SLOPE/W and SIGMA/W for evaluating slope stability and stress-deformation behavior, respectively. The numerical model was developed to replicate the field scenario at Chainage 24+200 on NH-148B (Bhiwani to Hansi), incorporating all relevant geotechnical parameters and boundary conditions derived from laboratory testing and field data.

Table 4.1: Material Properties Used in Seepage Analysis Model

Material Type	**Used in model**	**Saturated water content**	**Saturated Hydraulic Conductivity (k_x) (m/s)**	**Residual water content**	**Volumetric Water Content Function**	**Hydraulic Conductivity Function**
Silty Clay	Foundation	0.48	$1.5e^{-8}$	0.06	Van Genuchten	Van Genuchten
Silty Sand	Foundation	0.34	$1.3e^{-7}$	0.2	Van Genuchten	Van Genuchten
Poorly Graded Sand	Backfill	0.29	$5.1e^{-4}$	0.1	Van Genuchten	Van Genuchten
RE Wall (M35 Concrete)	RE Panel	_	Impermeable (No Flow)	_	Van Genuchten	Van Genuchten

Table 4.2 Material properties Used in Stability Analysis Model

S.No.	Material Model	Material Type	Unit weight (KN/m^3)	Cohesion (kpa)	Angle of internal friction (Φ)
1	Mohr-Coulomb	Silty Clay	20	102.98	24.5°
2	Mohr-Coulomb	Silty Sand	19.5	0.9	27.3°
3	Mohr-Coulomb	Poorly Graded Sand	17.89	0.139	35°

Table 4.3 Properties of Geo-Synthetics Used [13]

S.No.	Characterstics	Unit	Geogrid	Composite Geogrid
1	Ultimate strength	KN/m	80	80
2	Cross machine strength	KN/m	5	5
3	Elongation (longitudinal)	%	11	11
4	Pullout Resistance	Kpa	40	50
5	Tensile Capacity	KN	80	100
6	Polymer type		PET	PP[a], PET[b]
7	Thickness	mm	1.1	1.8[a], 1.1[b]
8	Mesh size	mm	426 × 51	426 × 51
9	Transmissivity	l/m h	-	3.8
10	Permittivity	l/m2 s	-	90

PET – Polyester, PP – polypropylene

4.3.1 SEEPAGE ANALYSIS

The seepage analysis for this study has been performed using SEEP/W, a module of GeoStudio 2018, which employs the Finite Element Method (FEM) to simulate groundwater flow through soil structures under transient and steady-state conditions. This analysis plays a vital role in evaluating how rainfall infiltration affects the pore water pressure, seepage paths, and overall stability of the geosynthetic-reinforced soil wall located at chainage 24+200 on NH-148B (Bhiwani to Hansi section).

The fundamental principle behind SEEP/W is based on Darcy's Law, which describes the rate of fluid flow through porous media. The law is mathematically expressed as:

$$Q = -kA(\frac{dh}{dl}) \tag{18}$$

where Q is the volumetric flow rate, k is the hydraulic conductivity, A is the cross-sectional area, and $\frac{dh}{dl}$ represents the hydraulic gradient. This equation forms the core of one-dimensional seepage evaluation.

For two-dimensional unsaturated flow, SEEP/W uses a modified form of Richards' Equation, which combines Darcy's law with the continuity equation to account for changes in water content over time. This equation is written as:

$$C(h).\frac{\partial h}{\partial t} = \frac{\partial}{\partial x}\left(k(h).\frac{\partial h}{\partial x}\right) + \frac{\partial}{\partial y}(k(h).\frac{\partial h}{\partial y}) \tag{19}$$

Here, C(h) = $\frac{d\theta}{dh}$ is the specific moisture capacity, k(h) is the unsaturated hydraulic conductivity, h is the pressure head, and q is the applied flux (such as rainfall). This partial differential equation is solved numerically using finite element discretization, allowing for accurate simulation of seepage under varying boundary and initial conditions.

The finite element formulation used by SEEP/W also considers the transient flow condition. The fundamental governing equation for transient two-dimensional seepage in FEM, as implemented in SEEP/W, is:

$$\frac{\partial}{\partial t}(m_w^2 \gamma_w h_t) = \frac{\partial}{\partial x}\left(-k_{wx}\frac{\partial h_t}{\partial x}\right) + \frac{\partial}{\partial y}\left(-k_{wy}\frac{\partial h_t}{\partial y}\right) + q \tag{20}$$

In this expression, m_w^2 is the slope of the Soil-Water Characteristic Curve (SWCC), γ_w is

the unit weight of water, h_t is the total hydraulic head, t is time, k_{wx} and k_{wy} are the hydraulic conductivity values in x and y directions respectively, and q is the external flux. To simulate unsaturated flow conditions, SEEP/W requires input of the Soil-Water Characteristic Curve (SWCC) and Hydraulic Conductivity Function (HCF). In this study, the van Genuchten model is employed to define the soil-water retention behavior:

$$\theta(h) = \theta_r + \frac{\theta_s - \theta_r}{[1 + (\alpha(h))^n]^m} \tag{21}$$

where θ(h) is the volumetric water content at a given pressure head h, θs is the saturated water content, θr is the residual water content, and α, n, m are fitting parameters with $m = 1 - \frac{1}{n}$.

To compute unsaturated hydraulic conductivity, the van Genuchten-based conductivity function is used:

$$k(h) = k_s S_e^l . [1 - (1 - S_e^{1/m})^m]^2 \tag{22}$$

where k(h) is the hydraulic conductivity at suction head h, k_s is the saturated conductivity, $S_e = \frac{\theta - \theta_r}{\theta_s - \theta_r}$ is the effective saturation, and l is a pore connectivity parameter.

The boundary conditions in the model include a non-ponding surface condition to simulate rainfall infiltration without surface water accumulation. Different flux values corresponding to rainfall intensities (15 mm/hr, 30 mm/hr, and 45 mm/hr) are applied as boundary fluxes. Initial conditions are defined based on field moisture content data.

This comprehensive seepage analysis provides an accurate understanding of how varying rainfall intensities influence pore pressure buildup, infiltration depth, and the potential for instability or deformation in the reinforced soil wall structure. The outputs from SEEP/W—such as pore water pressure contours, degree of saturation, and flow vectors—are essential for coupling with slope stability analysis and evaluating the overall performance of the reinforced system under adverse hydrological conditions.

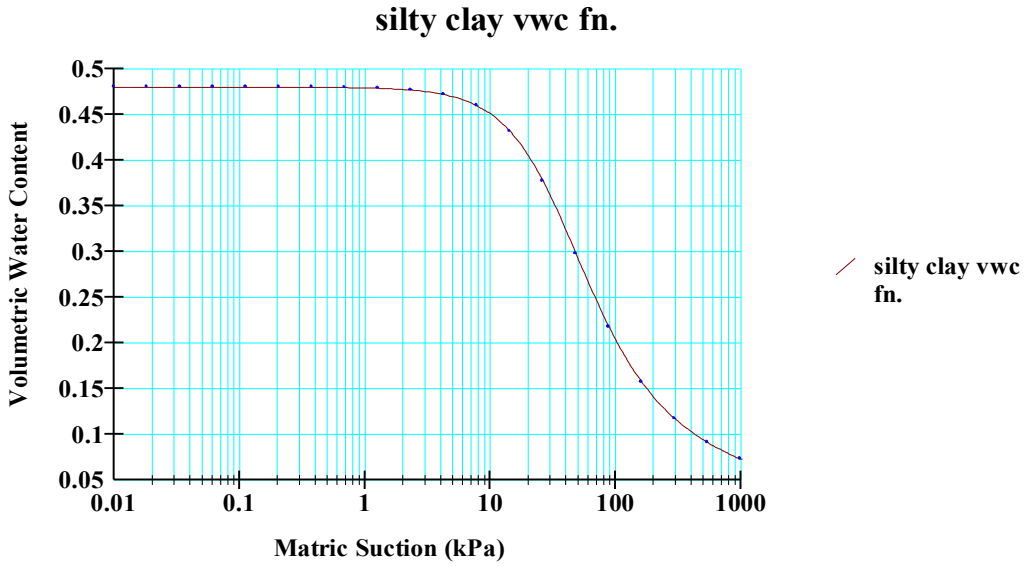

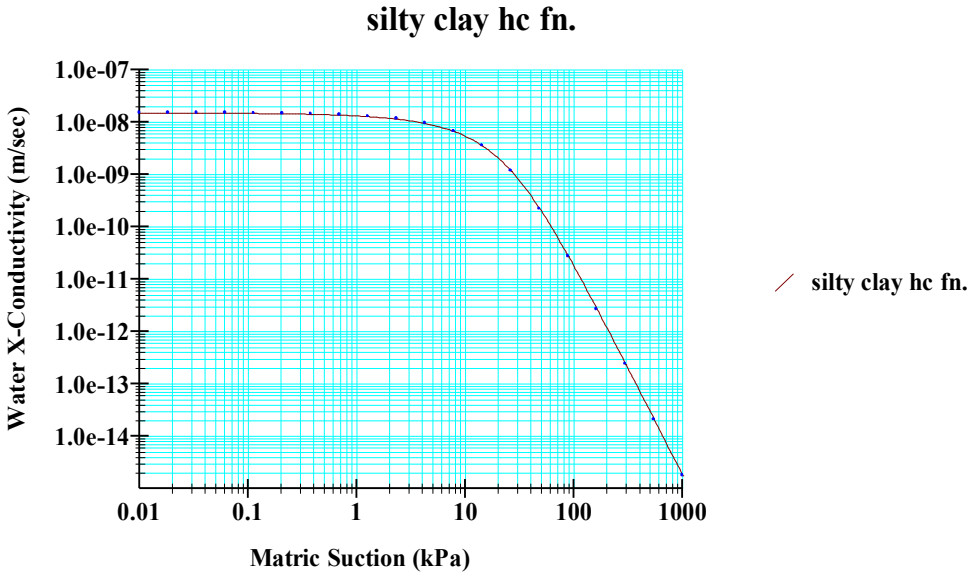

Figure 4.8 HCF for Silty Clay

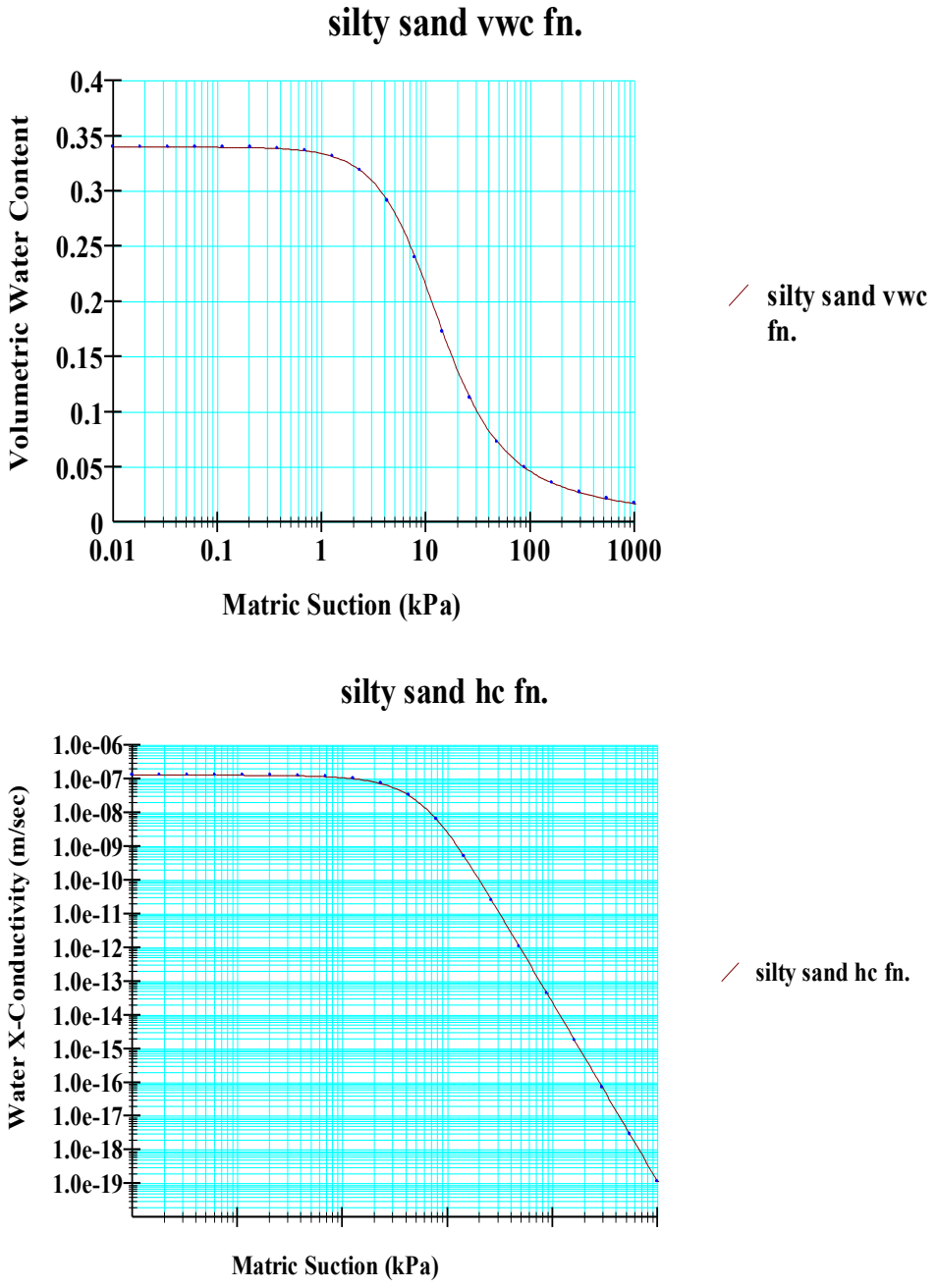

Figure 4.9 HCF and SWCC for Silty Sand

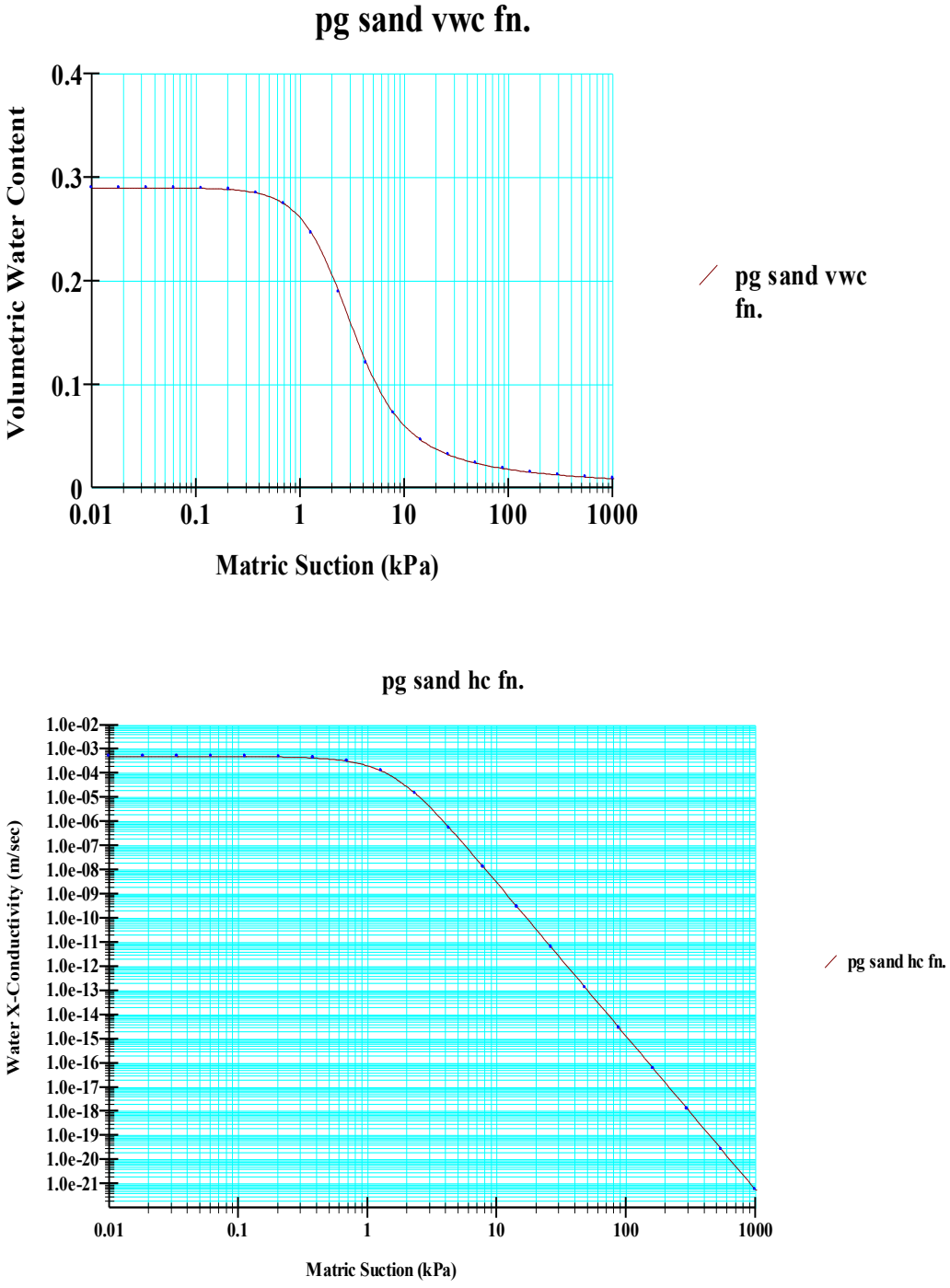

Figure 4.10 HCF and SWCC for Poorly Graded Sand

4.3.1.1 SEEPAGE ANALYSIS WITHOUT REINFORCEMENT

In this seep/w-analysis, a reinforced earth wall without geosynthetic reinforcement was simulated to assess its hydraulic behavior and stability under moderate rainfall using GeoStudio 2018's SEEP/W module. The 10-meter-high wall, constructed with M35 concrete RE panels, had poorly graded sand (SP) backfill over a foundation of 3.5 m silty sand (SM) and 2.5 m silty clay (ML). A 15 mm/hr rainfall intensity was applied as a flux boundary on the wall surface and backfill.

The groundwater table was modeled at 2 meters below ground level as a constant head boundary, influencing pore pressure and saturation within the soil. Unsaturated flow behavior was captured using the van Genuchten model for Soil-Water Characteristic Curves, along with soil-specific Hydraulic Conductivity and Volumetric Water Content Functions. These inputs enabled realistic simulation of pore pressure dynamics and infiltration in variably saturated soils.

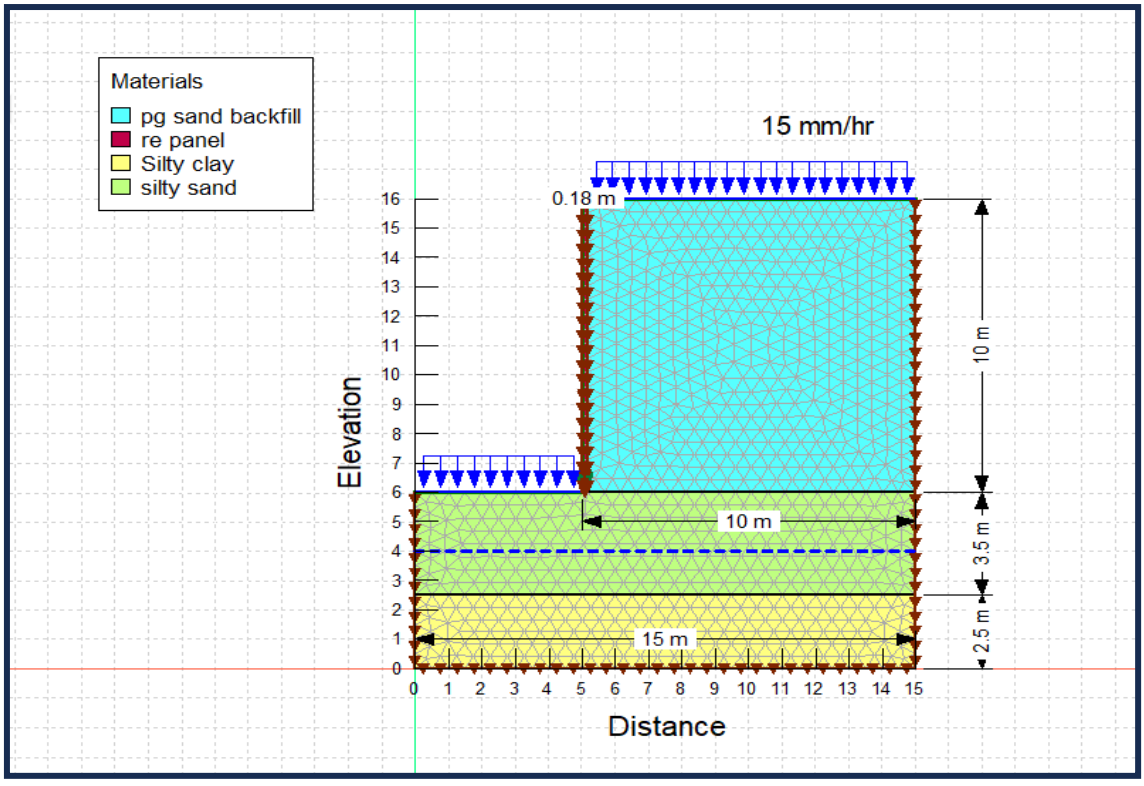

Figure 4.11 Reinforced Earth Wall without Reinforcement under moderate rainfall

4.3.1.2 SEEPAGE ANALYSIS WITH REINFORCEMENT

Geogrid Reinforcement

In the reinforced soil wall model, geogrid was incorporated as a primary tensile element to improve the overall stability and resistance against wall deformation. The geogrid was embedded at a horizontal length equal to 0.7H, where *H* is the total height of the reinforced wall (10 m). The pullout resistance of the geogrid is 40 kPa, while the tensile strength is 80 kN. A reduction factor of 2 was considered in accordance with standard design practices to account for long-term durability and installation effects. The inclusion of geogrid enhances soil-structure interaction and contributes significantly to resisting lateral earth pressures, especially under seepage and rainfall conditions.

Geocomposite Reinforcement

Alongside geogrid, geocomposite reinforcement was introduced to improve drainage and tensile resistance simultaneously. Similar to geogrid, geocomposite layers were also placed at 0.7H spacing. The pullout resistance of geocomposite is higher at 50 kPa, with a tensile capacity of 100 kN, providing both reinforcement and enhanced permeability characteristics. This dual-function material is particularly effective in controlling pore water pressure build-up during moderate rainfall conditions, modeled using the Van Genuchten function for unsaturated flow behavior and SEEP/W's hydraulic conductivity functions. Its role is critical in mitigating excess hydrostatic pressures and enhancing the overall stability of the wall.

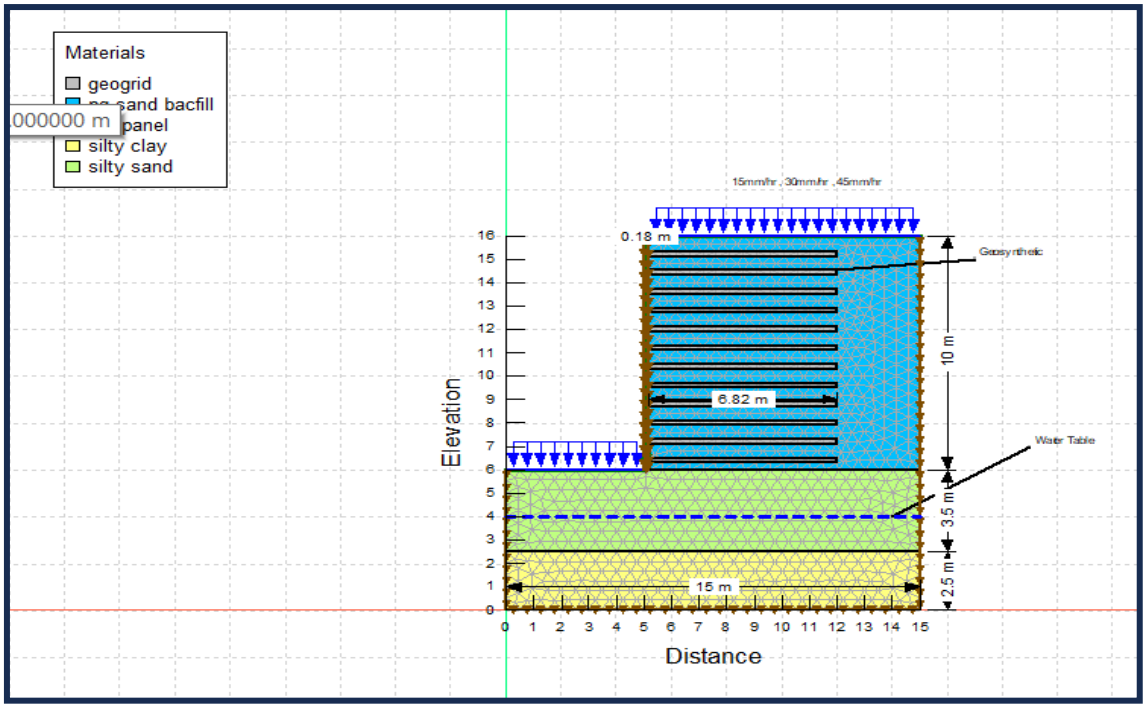

Figure 4.11 Geosynthetic Reinforced Soil Wall under Rainfall

4.3.2 STABILITY ANALYSIS

The stability analysis of the geosynthetic reinforced soil wall was performed using the SLOPE/W module of GeoStudio 2018, which applies the Morgenstern-Price method—a rigorous and widely accepted Limit Equilibrium Method (LEM). This method evaluates global slope stability by satisfying both force and moment equilibrium conditions, making it suitable for complex soil profiles and heterogeneous slope systems, such as the reinforced earth wall modelled in this study.

In this transient-coupled analysis, the pore water pressures generated from the SEEP/W seepage simulations (under different rainfall intensities) were imported into SLOPE/W to assess the wall's Factor of Safety (FOS) under rainfall-induced seepage conditions. The Morgenstern-Price method discretizes the slope into vertical slices and considers inter-slice forces governed by a user-defined function (commonly a half-sine distribution). This method is preferred due to its ability to analyze both simple and composite slip surfaces accurately, especially under complex loading and hydraulic conditions.

The shear strength of the soil is modelled using the Mohr-Coulomb failure criterion, expressed as:

$$\tau = c' + \sigma' \tan(\phi') \quad (22)$$

where:

- τ = shear strength of the soil,
- c' = effective cohesion,
- σ' = effective normal stress,
- ϕ' = effective angle of internal friction.

In unsaturated soils, the shear strength is influenced by **matric suction**, which can be incorporated using an extended form of the Mohr-Coulomb equation as proposed by Fredlund et al. (1978):

$$\tau = c' + (\sigma - u_a)\tan(\phi') + (u_a - u_w)\tan(\phi_b) \quad (23)$$

Where:

- u_a = pore air pressure (usually atmospheric = 0)
- u_w = pore water pressure
- ϕ_b = angle indicating the rate of increase in shear strength with matric suction

This extended formulation allows the **influence of negative pore water pressure (suction)** to be taken into account, particularly important for partially saturated zones in reinforced soil walls subjected to rainfall infiltration.

Soil parameters such as unit weight (γ), cohesion (c'), angle of internal friction (φ'), and pore pressure conditions are integrated into the model. The influence of infiltration from rainfall is modelled using unsaturated soil properties defined through the van Genuchten model and the volumetric water content function, linking directly with the hydraulic conductivity function (HCF) generated in SEEP/W.

This combined approach, rooted in the finite element seepage modelling and limit equilibrium stability analysis, provides a comprehensive assessment of the structural integrity and performance of the reinforced soil wall under variable hydrological conditions. The analysis adheres to standards outlined in IS:14458 and references foundational work from Fredlund & Rahardjo (1993) and GeoStudio documentation.

CHAPTER 5

RESULTS AND DISCUSSIONS

5.1 EXPERIMENTAL RESULTS

5.1.1 GRAIN SIZE DISTRIBUTION ANALYSIS

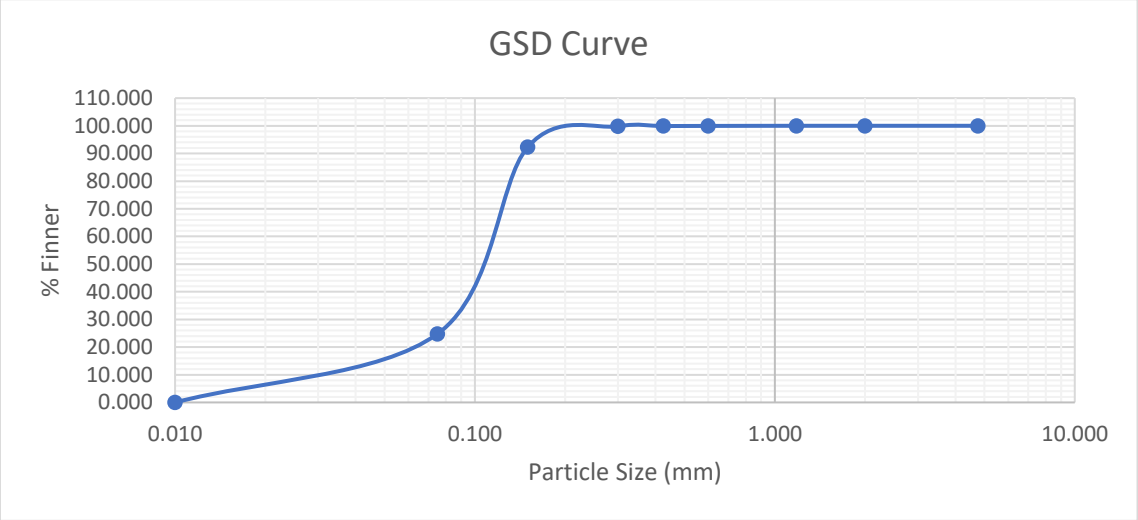

Figure 5.1 Grain Size Distribution Analysis Curve

Table 5.1 Uniformity Coefficient and Curvature Coefficient of soil sample

Parameters	**Values**
D10 (mm)	0.029
D30 (mm)	0.083
D60 (mm)	0.129
Uniformity Coefficient $Cu = D_{60}/D_{10}$	**4.448**
Curvature Coefficient $Cc=D_{30}^2 / (D_{60} \times D_{10})$	**1.841**
Soil Type	**Poorly Graded Sand**

5.1.2 SPECIFIC GRAVITY TEST

Table 5.2 Specific Gravity of Soil Specimen

Parameters	Notations	Units	Specimen 1	Specimen 2
Weight of Density Bottle empty	**W_1**	**gm**	35.513	35.366
Empty Density Bottle + Dry Soil	**W_2**	**gm**	41.520	41.375
Empty Density Bottle + Dry Soil +Water	**W_3**	**gm**	89.774	89.397
Empty Density Bottle + Water	**W_4**	**gm**	86.036	85.711
Specific Gravity	**Gs**		**2.647**	**2.587**

Average value of specific gravity of Soil sample = (2.50 + 2.77 + 2.63)/3 **= 2.63**

5.1.3 MODIFIED PROCTOR TEST

Table 5.3 Dry Density and Moisture Content relation for Modified Proctor Test

S.No.	Dry Density, γ_d (kN/m^2)	Moisture Content, w (%)
1	17.395	5.999
2	17.540	7.788
3	17.832	9.775
4	17.875	11.685
5	17.651	13.795
6	17.111	15.633

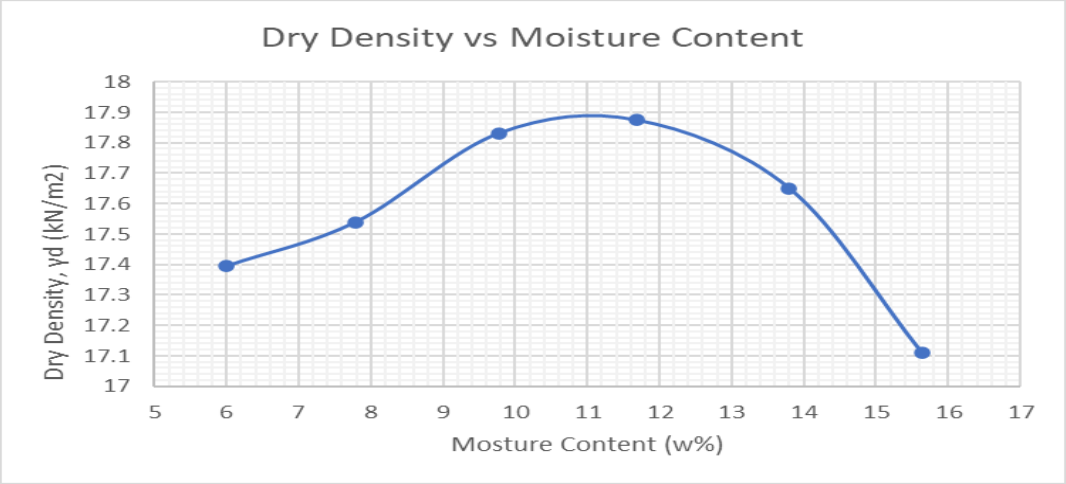

Figure 5.2 Dry Density and Moisture Content Curve

Table 5.4 Results of Modified Proctor Test Results

Parameters	**Optimum Moisture Content (%)**	**Maximum Dry Density (kN/m^2)**	**Bulk Density (kN/m^2)**
Soil Specimen	11%	17.89	19.86

5.1.4 Constant Head permeability Test

Table 5.5 Observations and Results of Constant Head Permeability Test

Trial	**Length of Specimen (cm)**	**Cross-Sectional Area (cm^2)**	**Time (sec)**	**Discharge (ml)**	**Head difference (cm)**	**Permeability (cm/sec)**
1	15	50.3	60	1125	30	0.047
2	15	50.3	60	1235	30	0.052
3	15	50.3	60	1310	30	0.055
Average Permeability (cm/sec)						**0.051**

5.1.4 DIRECT SHEAR TEST

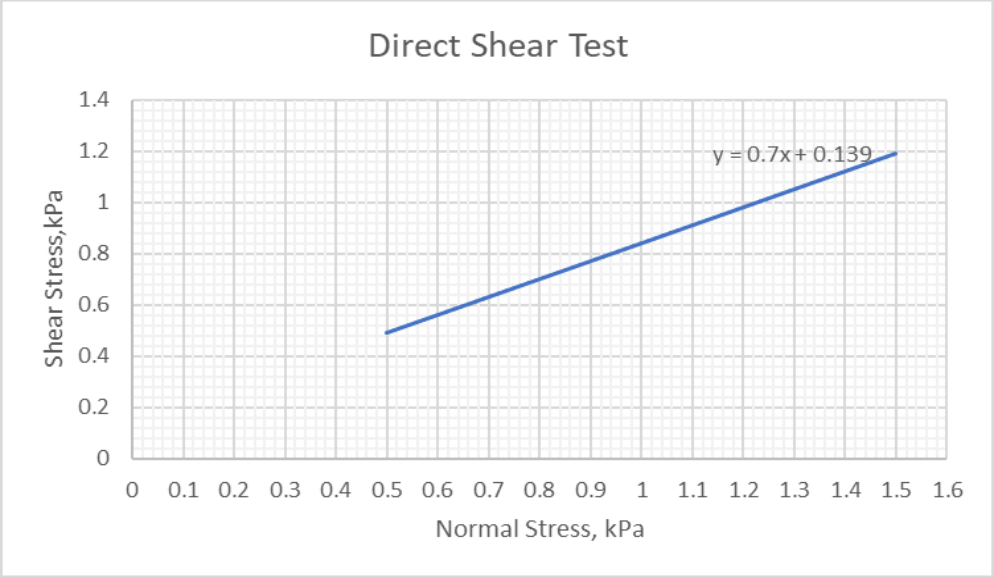

Figure 5.3 Mohr- Coulomb Failure envelope

Table 5.6 Values of cohesion (c) and internal friction angle (φ)

Cohesion (kg/cm^2)	0.139
Angle of Internal Friction (˚)	35˚

Table 5.7 Showing values of different soil properties

S.No.	**Soil Property**	**Value**
1	Soil Classification	SP
2	Natural Water Content (%)	4.58
3	Bulk Unit Weight (γ_b) (kN/m^3)	19.86
4	Maximum Dry Density (γ_d) (kN/m^3)	17.89
5	Saturated Unit Weight (γ_{sat}) (kN/m^3)	21.13
6	Coefficient of permeability (cm/sec)	0.051
7	Cohesion (kg/cm^2)	0.139
8	Angle of internal friction (φ°)	35˚

5.2 EXPERIMENTAL MODELLING OF REINFORCED EARTH WALL RESULTS

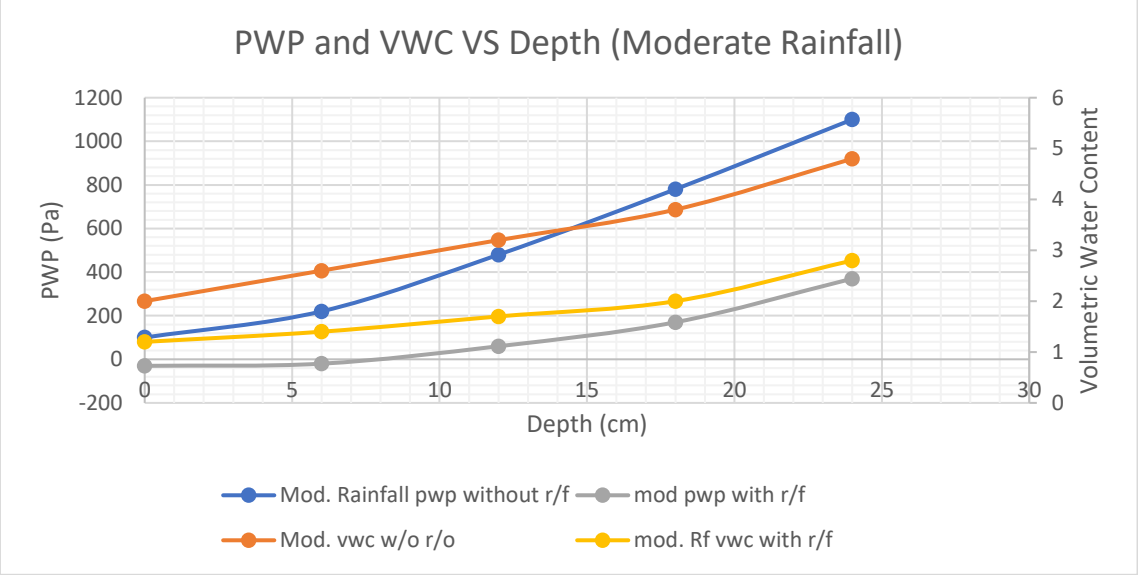

Figure 5.4 PWP and VWC vs Depth Relationship with or without Reinforcement under Moderate Rainfall

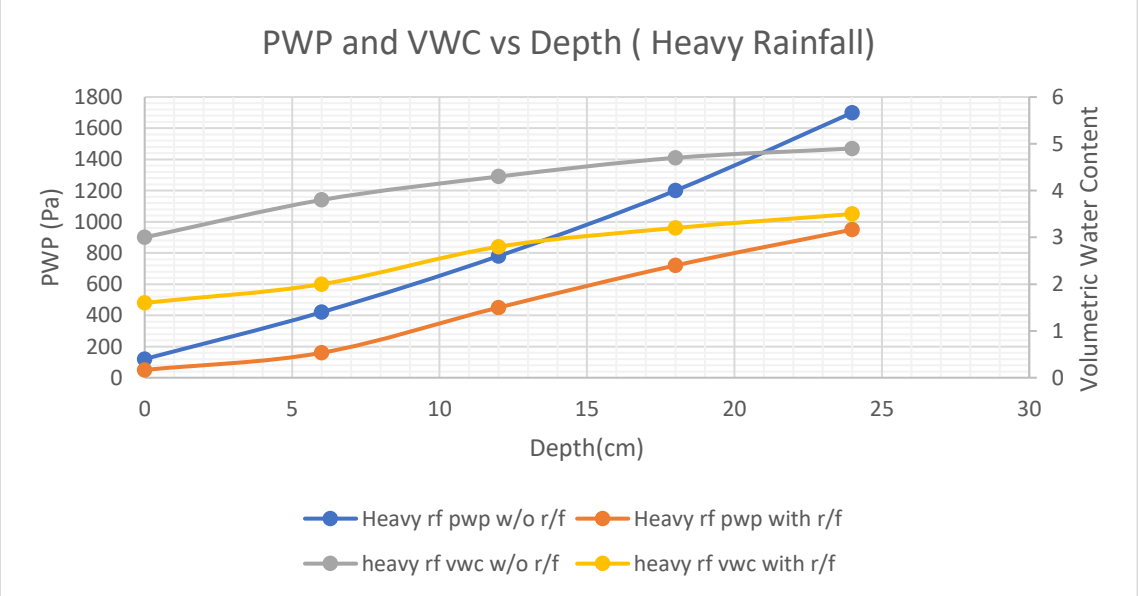

Figure 5.5 PWP and VWC vs Depth Relationship with or without Reinforcement under Heavy Rainfall

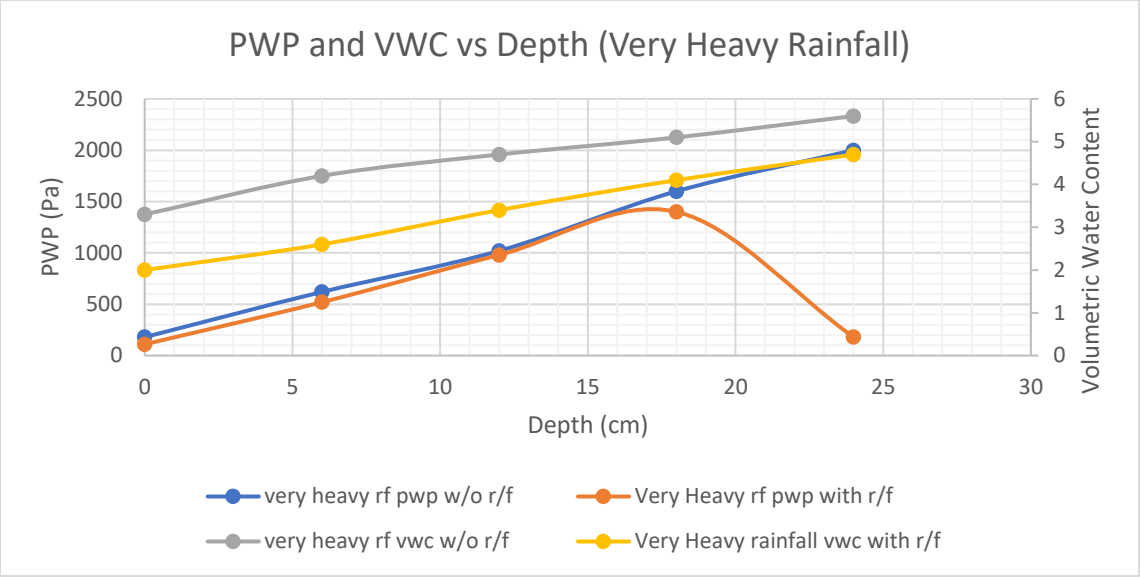

Figure 5.6 PWP and VWC vs Depth Relationship with or without Reinforcement under Very Heavy Rainfall

Based on the experimental model data under various rainfall intensities, the geosynthetic-reinforced soil wall demonstrated significantly better performance than the unreinforced wall:

Under very heavy rainfall, the pore water pressure (PWP) at 24 cm depth was reduced from 2000 Pa (unreinforced) to 1800 Pa (reinforced), and volumetric water content (VWC) decreased from 5.6% to 4.7%.

In heavy rainfall, PWP dropped from 1700 Pa to 950 Pa, and VWC from 4.9% to 3.5% at 24 cm depth.

For moderate rainfall, the effect was even more significant—PWP reduced from 1100 Pa to 370 Pa, and VWC from 4.8% to 2.8% at the same depth.

Overall, the inclusion of geosynthetics effectively reduced water-induced stresses and improved drainage, enhancing the wall's stability across all rainfall intensities.

5.3 NUMERICAL MODELLING

5.3.1 SEEPAGE ANALYSIS (SEEP/W)

a) VOLUMETRIC WATER CONTENT VARIATION WITH TIME UNDER DIFFERENT RAINFALL INTENSITIES

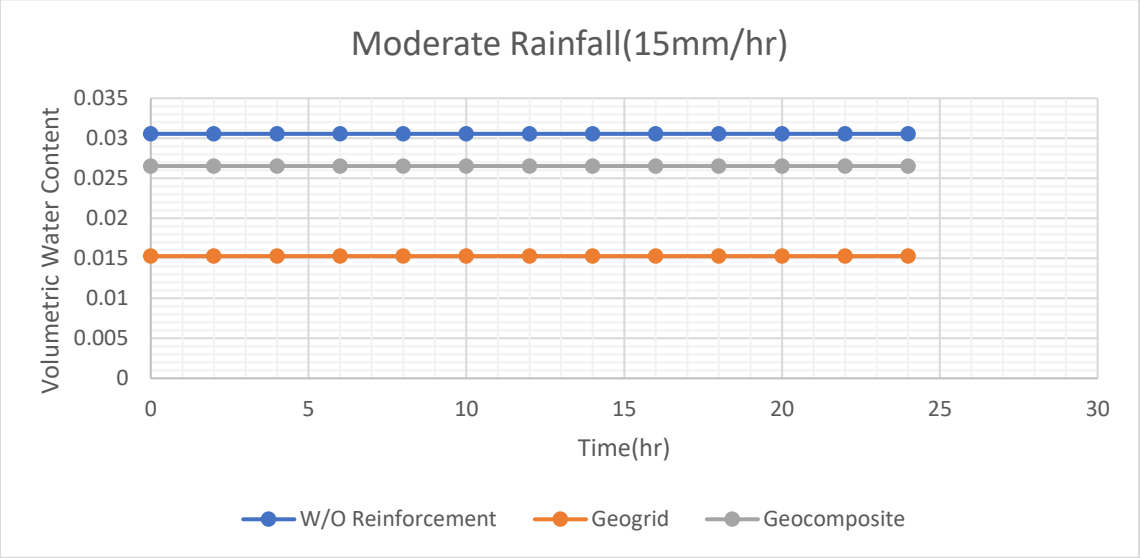

Figure 5.7 Variation of Volumetric Water Content with Time under Moderate Rainfall

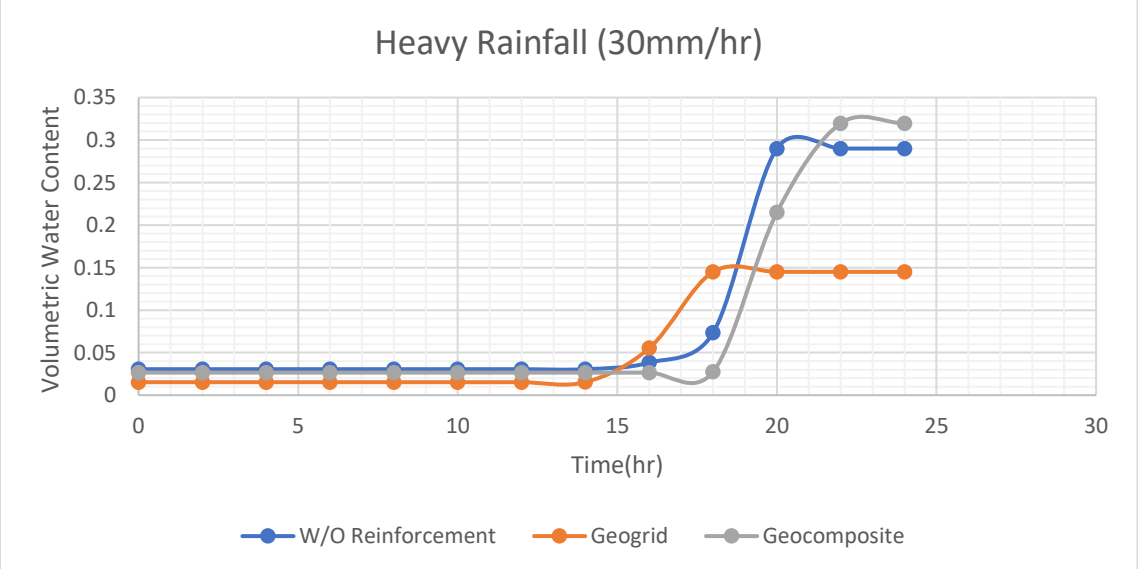

Figure 5.8 Variation of Volumetric Water Content with Time under Heavy Rainfall

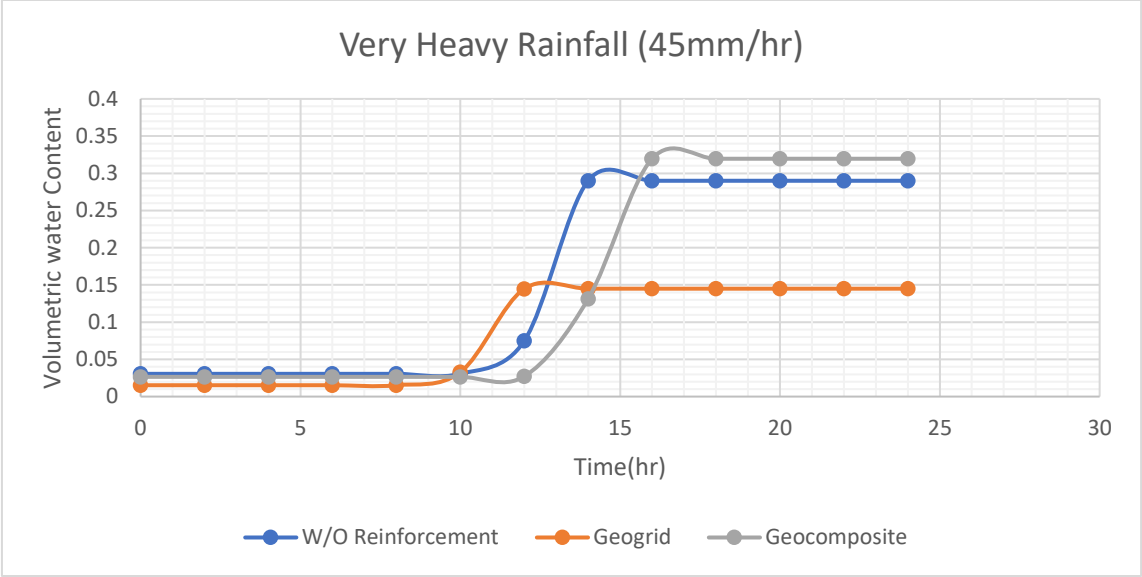

Figure 5.9 Variation of Volumetric Water Content with Time under Heavy Rainfall

b) PORE WATER VARIATION WITH TIME UNDER DIFFERENT RAINFALL INTENSITIES

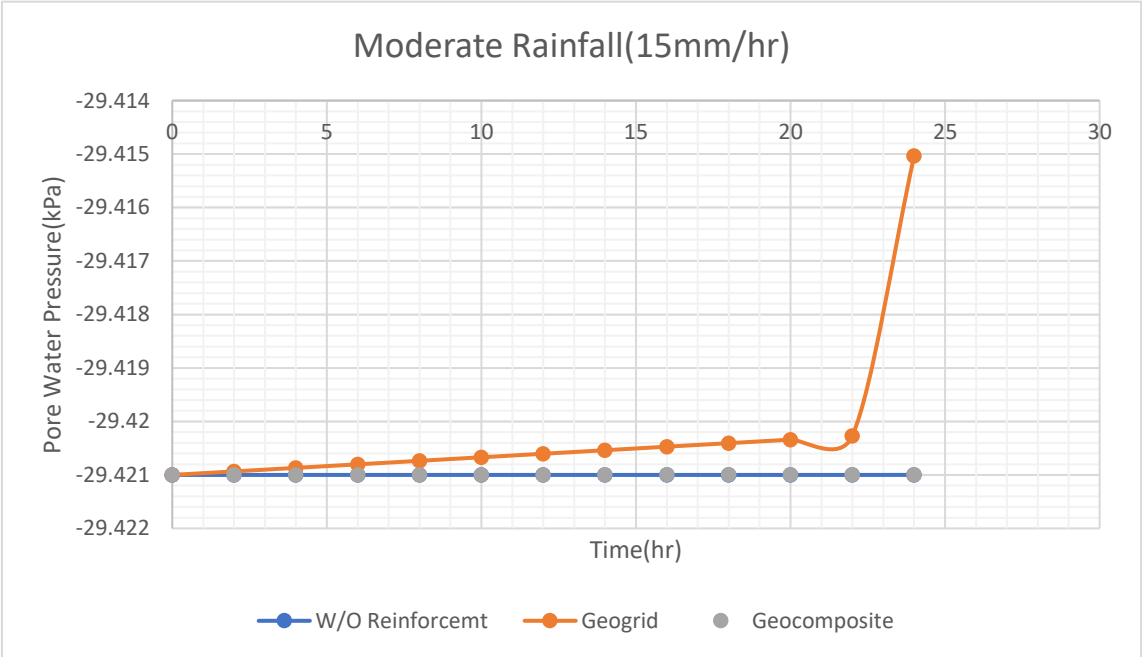

Figure 5.10 Variation of Pore Pressure with Time under Moderate Rainfall

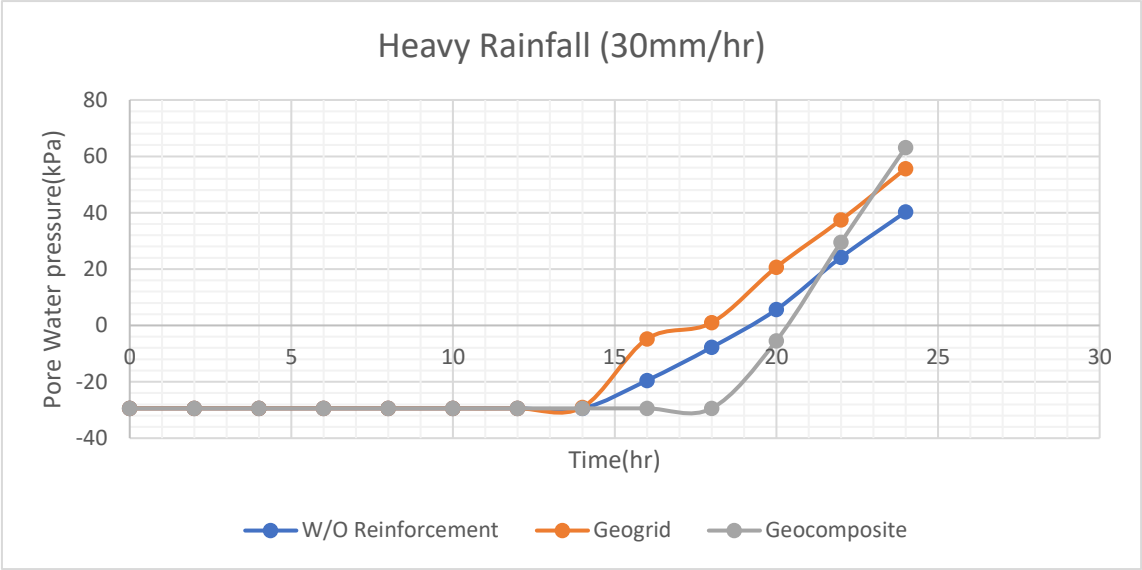

Figure 5.11 Variation of Pore Pressure with Time under Heavy Rainfall

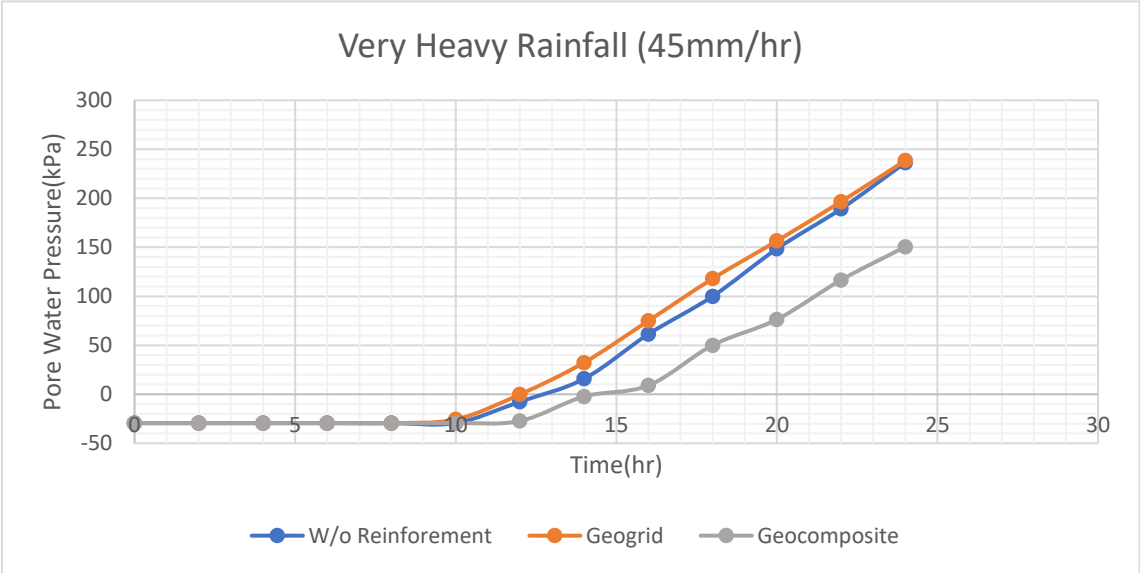

Figure 5.12 Variation of Pore Pressure with Time under Very Heavy Rainfall

Table 5.8 Summary of Seepage Parameters under Different Rainfall and Reinforcement Conditions

Rainfall Intensity	**Condition**	**Volumetric Water Content (% at 24 hr)**	**Pore Pressure (kPa at 24 hr)**
Moderate Rainfall (15mm/hr)	Without Reinforcement	0.3060	-29.42
	Geogrid	0.0153	-29.415
	Geocomposite	0.0265	-29.42
Heavy Rainfall (30mm/hr)	Without Reinforcement	0.2900	40.28
	Geogrid	0.1450	55.66
	Geocomposite	0.3196	63.13
Very Heavy Rainfall (45mm/hr)	Without Reinforcement	0.2900	236.37
	Geogrid	0.1450	238.53
	Geocomposite	0.3196	150.49

Under moderate rainfall, the unreinforced wall showed a gradual increase in volumetric water content (3.06%) with sustained negative pore pressure (-29.42 kPa), indicating limited infiltration but low resistance to moisture accumulation. The geogrid-reinforced wall further reduced water content to 1.53% while maintaining the same pore pressure, suggesting improved drainage due to reinforcement layers. In contrast, the geocomposite wall showed slightly higher water content (2.65%) but stable pore pressure (-29.42 kPa), highlighting its capacity to evenly distribute moisture while ensuring suction stability. Under heavy rainfall, the unreinforced wall saturated rapidly (VWC: 29%, PWP: 40.28 kPa), while geogrid reduced saturation (14.5%) but showed higher pore pressure (55.66 kPa), indicating partial seepage control. The geocomposite wall effectively handled excess water, though water content was highest (31.96%), it maintained stable pore pressure

(63.13 kPa), proving its high permeability. Under very heavy rainfall, the unreinforced wall faced excessive pore pressure build-up (236.37 kPa), while the geogrid wall peaked even higher (238.53 kPa), signaling poor dissipation. In contrast, the geocomposite wall sustained the same water content but limited pore pressure to 150.49 kPa, confirming superior drainage capacity and improved wall stability. These outcomes affirm that geocomposite reinforcements offer optimal seepage reduction and structural stability across varying rainfall intensities.

5.3.2 STABILITY ANALYSIS (SLOPE/W)

5.3.2.1 WITHOUT REINFORCEMENT

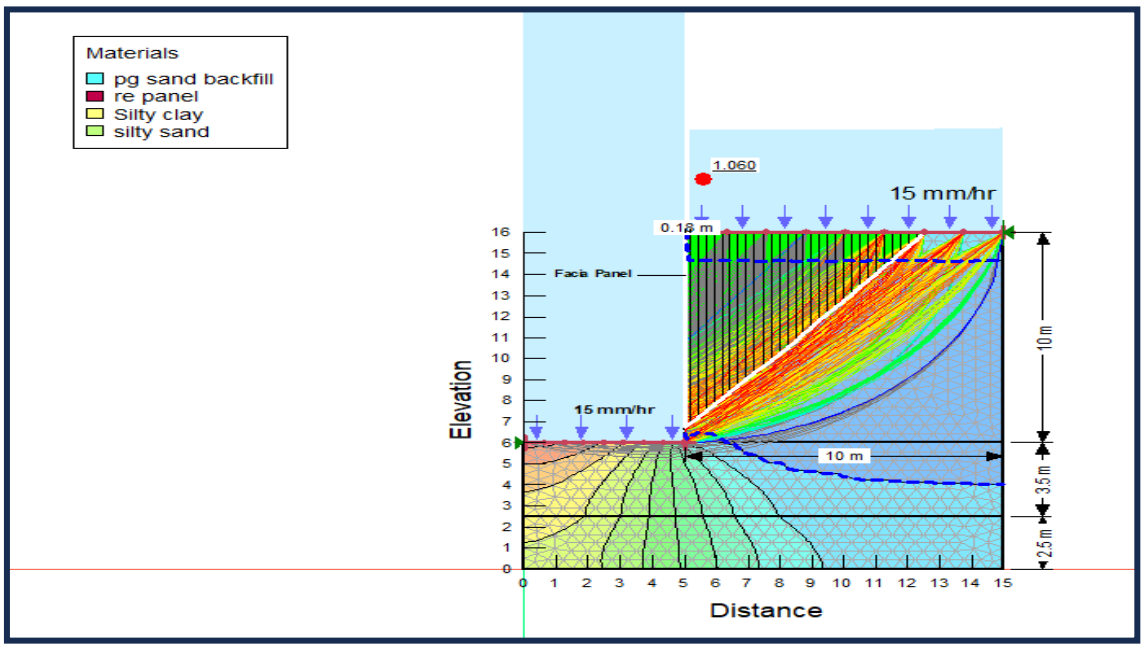

Figure 5.13 Reinforced Earth Wall without reinforcement under moderate rainfall F.O.S less than 1.3

As per IS 14458 (Part 2): 1997 – Retaining Walls for Hill Areas – Guidelines, and IRC SP 102:2024 & FHWA-NHI-10-024– guidelines for design and construction of reinforced soil walls, a minimum Factor of Safety (F.O.S) of 1.3 is required for the safe performance of retaining structures under seepage or saturated conditions. In the present study, under a moderate rainfall intensity of 15 mm/hr sustained for 24 hours, the unreinforced earth

retaining wall yielded an F.O.S of 1.06, which is significantly below the required safety limit. This result indicates that the wall is unstable and prone to failure under rainfall-induced seepage conditions, primarily due to the rise in pore water pressures and consequent reduction in soil shear strength.

To mitigate this risk and enhance structural performance, geogrid reinforcement was introduced and analyzed under multiple rainfall intensities. The results showed a substantial improvement in slope stability, with the F.O.S increasing beyond the IS-recommended value of 1.3 across all scenarios. The geogrid effectively mobilized tensile resistance within the backfill, reduced deformations, and enhanced the overall safety of the structure, confirming its efficacy in preventing rainfall-induced failures in reinforced earth walls.

5.3.2.1 WITH REINFORCEMENT (GEOGRID)

a) MODERATE RAINFALL

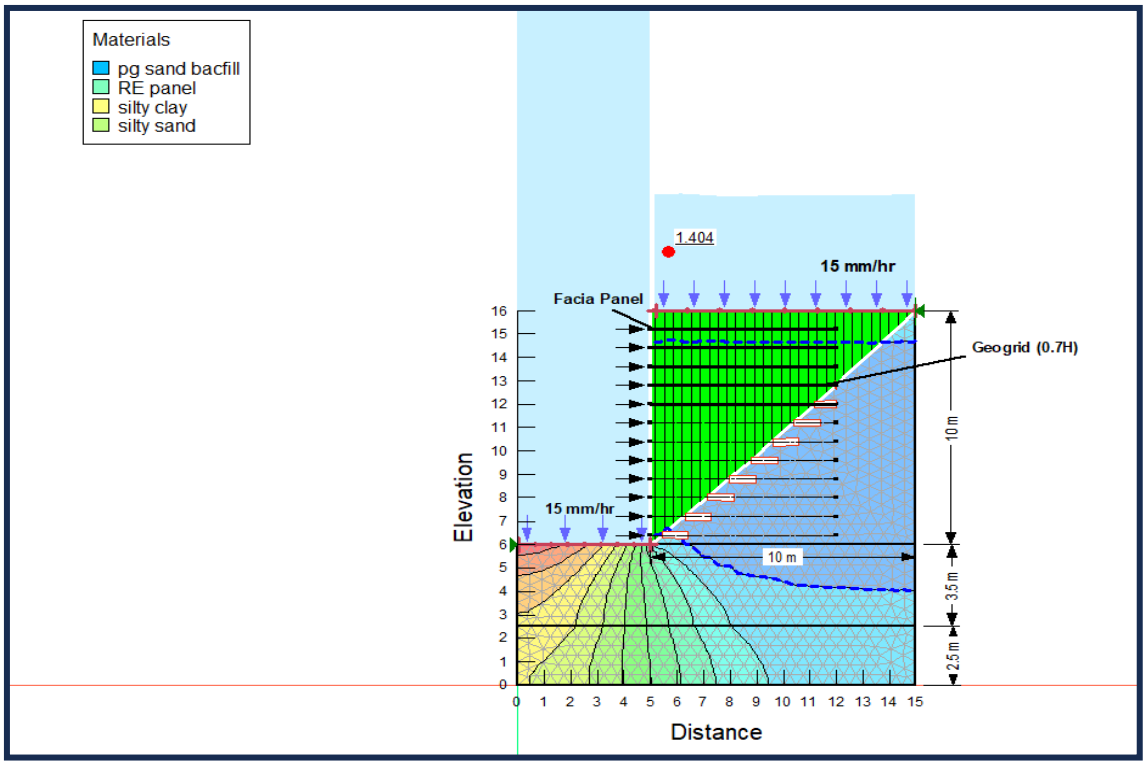

Figure 5.14 Reinforced Earth Wall with reinforcement (Geogrid) under moderate rainfall F.O.S more than 1.3

b) HEAVY RAINFALL

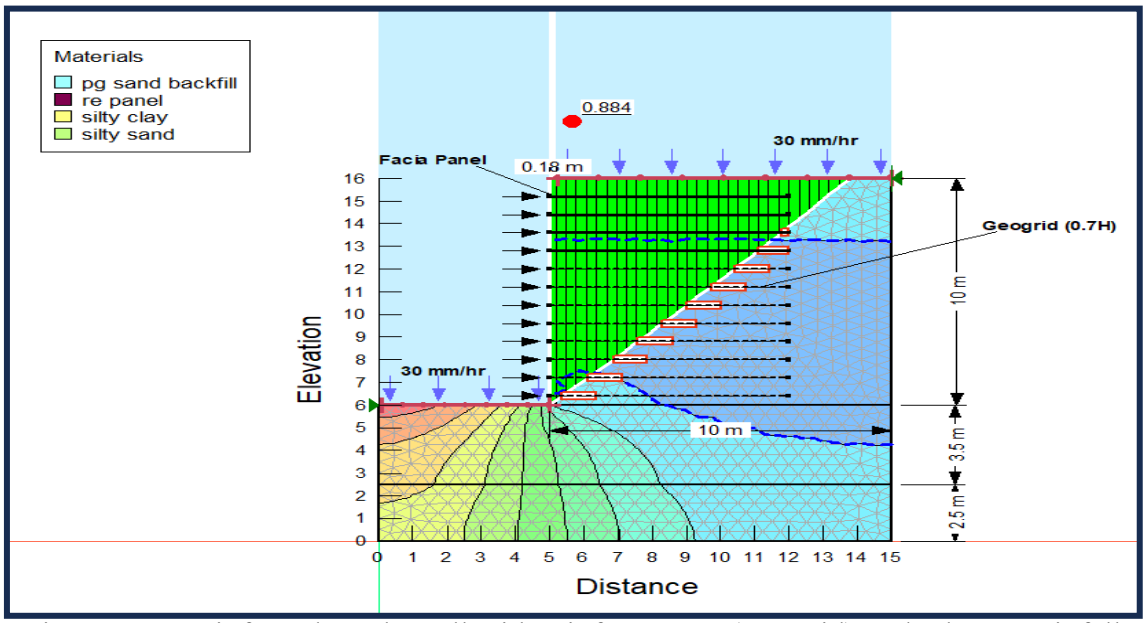

Figure 5.15 Reinforced Earth Wall with reinforcement (Geogrid) under heavy rainfall F.O.S less than 1.3

In this study, a geogrid with a mesh size of 426 mm × 51 mm and a tensile strength of 80 kN/m was used to reinforce the earth wall. Under moderate rainfall intensity (15 mm/hr), the reinforced wall achieved a Factor of Safety (F.O.S) of 1.404, which is greater than the minimum required value of 1.3 as per IRC SP 102:2024 & FHWA-NHI-10-024, indicating satisfactory stability. However, under heavy rainfall conditions (30 mm/hr), the F.O.S reduced significantly to 0.884, rendering the wall unsafe due to increased seepage pressures. To improve performance, a geocomposite with the same mesh size (426 mm × 51 mm) and a higher tensile strength of 100 kN/m, along with superior drainage characteristics, was implemented. The geocomposite-reinforced wall successfully maintained F.O.S above 1.3 across all rainfall intensities, demonstrating enhanced resistance to rainfall-induced instability through improved drainage and tensile reinforcement.

5.3.2.2 WITH REINFORCEMENT (GEOCOMPOSITE)

a) MODERATE RAINFALL

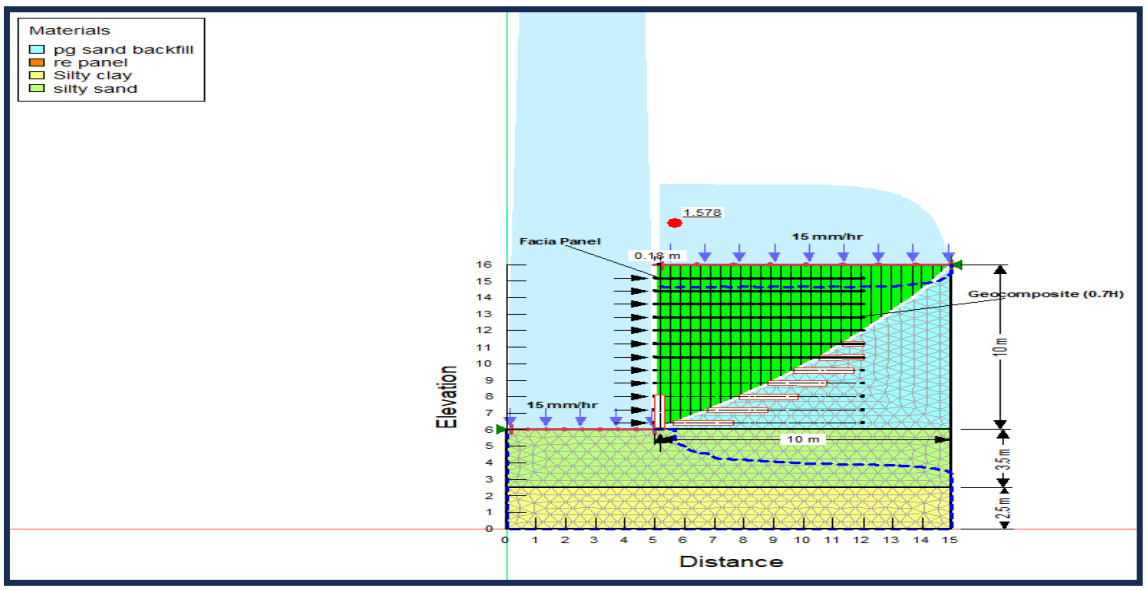

Figure 5.16 Reinforced Earth Wall with reinforcement (Geocomposite) under moderate rainfall F.O.S more than 1.3

b) HEAVY RAINFALL

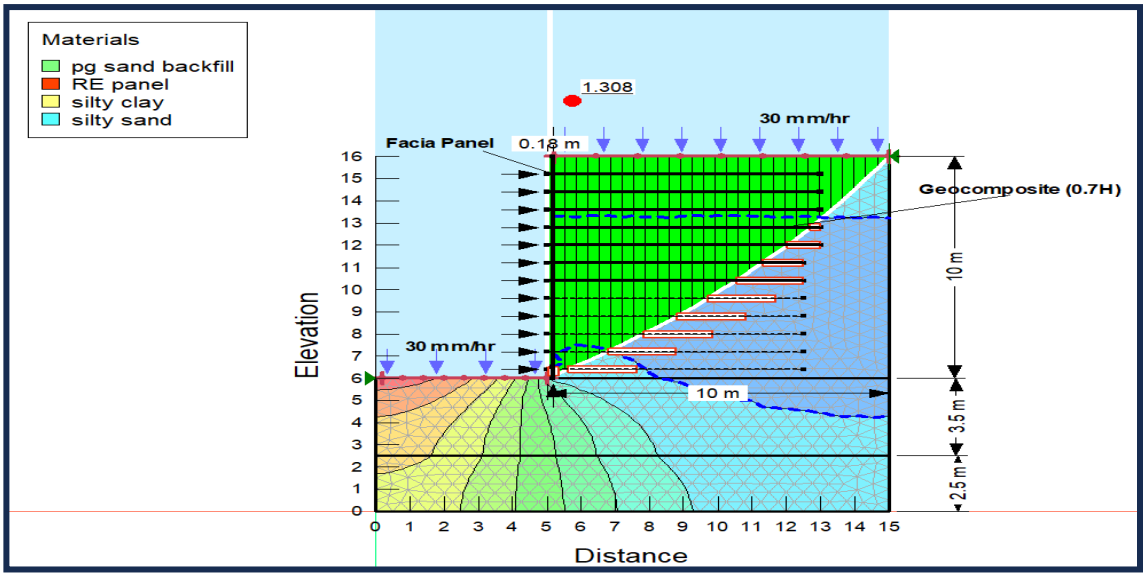

Figure 5.17 Reinforced Earth Wall with reinforcement (Geocomosite) under heavy rainfall F.O.S more than 1.

c) VERY HEAVY RAINFALL

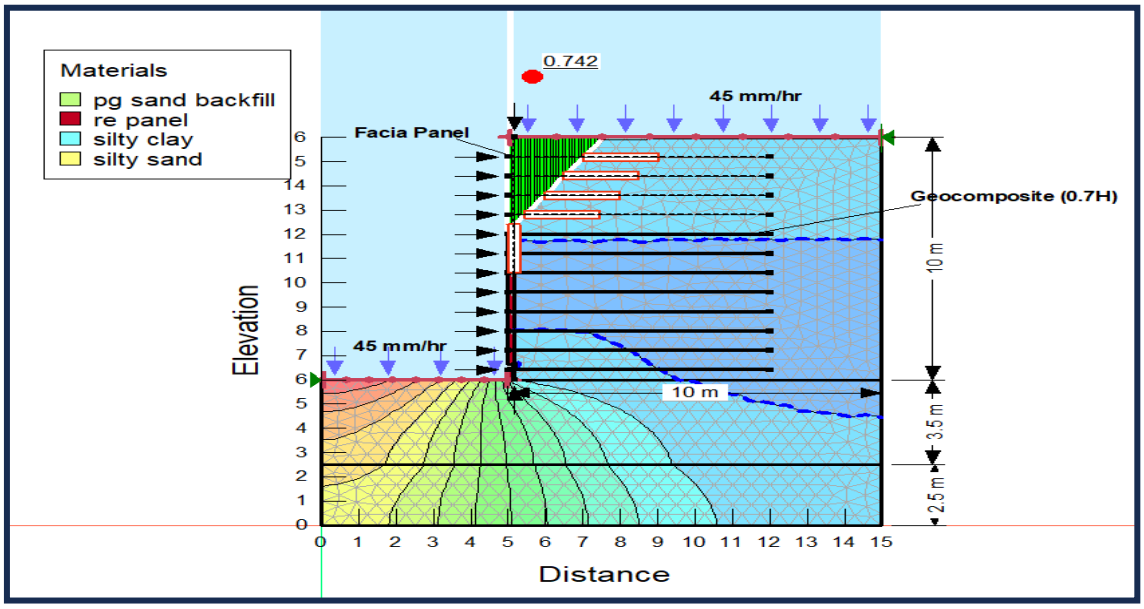

Figure 5.18 Reinforced Earth Wall with reinforcement (Geocomosite) under very heavy rainfall F.O.S less than 1.3

A geocomposite with a tensile strength of 100 kN/m, transmissivity of 3.8 L/m·h, and permittivity of 90 L/m²·s was used to reinforce the earth wall. Under moderate (15 mm/hr) and heavy rainfall (30 mm/hr) for 24 hours, the wall showed F.O.S values of 1.578 and 1.308, respectively—both above the IS 6403:1981 safety limit of 1.3, indicating stable performance. However, under very heavy rainfall (45 mm/hr), the F.O.S dropped to 0.742, indicating instability. To improve safety, parameters such as increasing geocomposite length, using higher-strength materials, and reducing reinforcement spacing to 400 mm can be applied. These enhancements, illustrated in Figure 5.14, aim to achieve stability even under extreme rainfall conditions.

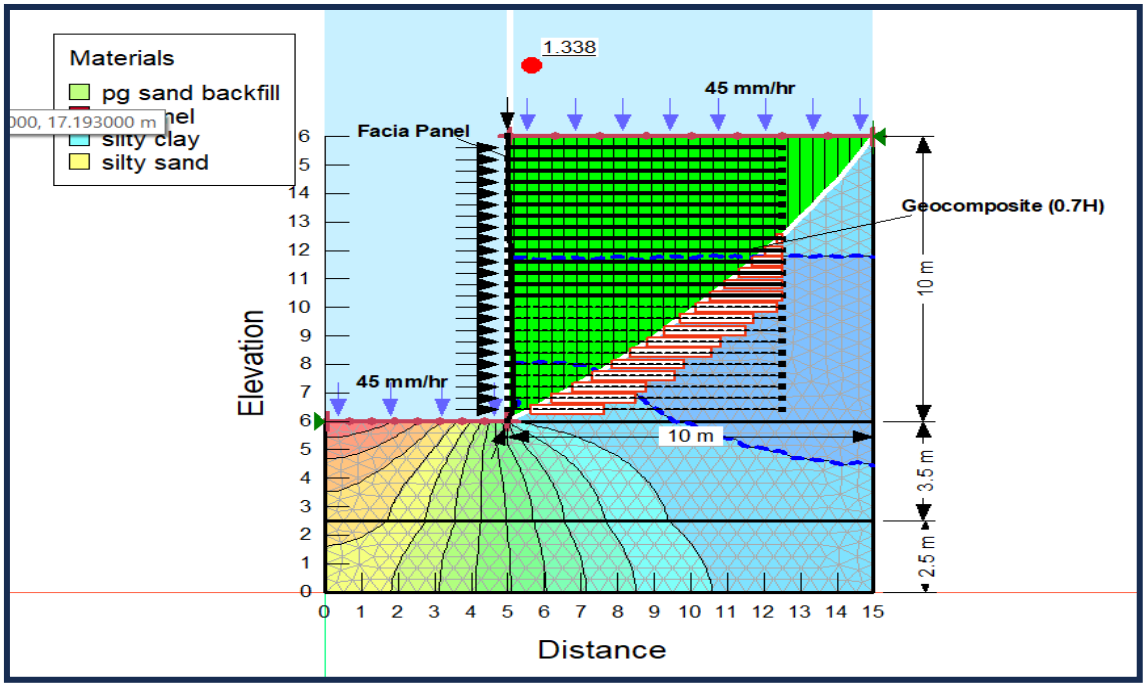

Figure 5.19 Reinforced Earth Wall with reinforcement (Geocomosite) under very heavy rainfall F.O.S greater than 1.3

To enhance stability under very heavy rainfall (45 mm/hr), the tensile strength of the geocomposite was increased from 100 kN/m to 160 kN/m, representing a 60% increase. Additionally, the length of the geocomposite was extended from 7.0 m to 7.5 m, resulting in a 7.14% increase, and the reinforcement was introduced at 400 mm vertical spacing. With these modifications, the Factor of Safety improved to 1.338, exceeding the minimum requirement of 1.3 as per IRC SP 102:2024 & FHWA-NHI-10-024, and confirming the wall's stability under extreme rainfall conditions.

CHAPTER 6

CONCLUSIONS

To ensure the structural safety and long-term performance of a 10 m high and 10 m long geosynthetic-reinforced soil wall with a 6 m foundation, a comprehensive study was conducted involving both scaled experimental modeling (1:30) and numerical analysis (SEEP/W and SLOPE/W) under varying rainfall intensities: moderate (15 mm/hr), heavy (30 mm/hr), and very heavy (45 mm/hr).

- Experimental results indicated that under very heavy rainfall, the unreinforced wall recorded a PWP of 2000 Pa and VWC of 5.6% at 24 cm depth. These values were reduced to 1800 Pa and 4.7%, respectively, with reinforcement—demonstrating improved drainage and reduced saturation.
- In moderate rainfall conditions, reinforcement reduced PWP from 1100 Pa to 370 Pa and VWC from 4.8% to 2.8%, confirming the effectiveness of reinforcement in minimizing moisture buildup.
- Numerical seepage analysis showed comparable trends: under moderate rainfall, the unreinforced wall exhibited a VWC of 30.6% and negative PWP (-29.42 kPa), indicating unsaturated conditions. With geogrid and geocomposite, VWC dropped to 1.53% and 2.65%, respectively, while PWP remained stable at approximately -29.42 kPa, highlighting enhanced drainage and suction.
- Under heavy rainfall, PWP increased to 40.28 kPa (unreinforced), 55.66 kPa (geogrid), and 63.13 kPa (geocomposite), with corresponding VWC values of 29.0%, 14.5%, and 31.96%. In very heavy rainfall, PWP reached 236.37 kPa (unreinforced) and 238.53 kPa (geogrid), while geocomposite limited it to 150.49 kPa despite high VWC—demonstrating better dissipation.
- Stability analysis revealed an unreinforced Factor of Safety (F.O.S) of 1.06 under moderate rainfall—below the IRC SP 102:2024 & FHWA-NHI-10-024 minimum requirement of 1.3. Geogrid reinforcement improved F.O.S to 1.404 under moderate but dropped to 0.884 under heavy rainfall. Geocomposite

reinforcement consistently maintained F.O.S above 1.3 under moderate (1.578) and heavy (1.308) rainfall.

- For very heavy rainfall, F.O.S initially dropped to 0.742 with geocomposite, but after optimizing the tensile strength to 160 kN/m, increasing length to 7.5 m, and reducing vertical spacing to 400 mm, stability was restored with an F.O.S of 1.338.

Both experimental and numerical analyses confirm that geosynthetics—particularly geocomposites—significantly reduce seepage effects and enhance the structural stability of reinforced soil walls under varied rainfall intensities. The close agreement between experimental trends and numerical outputs validates the reliability of the modeling approach and supports the use of geosynthetics as an effective drainage and reinforcement solution in earth-retaining systems.

REFERENCES

[1] W. Zou, " Hydromechanical behaviors of geogrids-reinforced expansive soil slopes: Case study and numerical simulation," *ELSEVIER (Computers and Geotechnics),* vol. 174, p. 18, 2024.

[2] J.-C. Liu, "Investigation on failure of deep excavations in erodible sandy strata triggered by heavy rainfall," *Engineering Failure Analysis ,* vol. 164, p. 21, 2024.

[3] F. Chi, "Stochastic seepage analysis in embankment dams using different types of random fields," *Computers and Geotechnics,* vol. 162, p. 13, 2023.

[4] H. Guo, " Three-dimensional numerical analysis of plant-soil hydraulic interactions on pore water pressure of vegetated slope under different rainfall patterns," *Journal of Rock Mechanics and Geotechnical Engineering,* vol. 16, p. 11, 2024.

[5] S. Chaiprakaikeow, "Field evaluation of moisture-suction regime and modulus of geosynthetic-reinforced soil wall with geo-composite side-drain," *Geotextiles and Geomembranes,* vol. 52, p. 14, 2024.

[6] C. Zhu, "Evaluation on wetting effect of loess high-fill embankment under rainfall and groundwater uplift," *Transportation Geotechnics ,* vol. 38, p. 19, 2023.

[7] X.-k. Li, "Thermal-seepage coupled numerical simulation methodology for the artificial ground freezing process," *Computers and Geotechnics ,* vol. 156, p. 9, 2023.

[8] J. C. Guzma´n-Martı´nez, " Effects of hydro-mechanical material parameters on the capillary barrier of reinforced embankments," *ScienceDirect,* vol. 62, p. 17, 2022.

[9] J. Xu, "Numerical modeling of seepage and deformation of unsaturated slope subjected to post-earthquake rainfall," *Computers and Geotechnics ,* vol. 148, p. 17, 2022.

[10] X. B. Xu, "Seepage failure of a foundation pit with confined aquifer layers and its reconstruction," *Engineering Failure Analysis,* vol. 138, p. 13, 2022.

[11] K. Wang, "Research on stability of steep bank slope and reserved thin-walled rock

cofferdam during excavation of intake foundation pit," *Engineering Failure Analysis ,* vol. 141, p. 21, 2022.

[12] G. Nunes, "Numerical study of the impact of climate conditions on stability of geocomposite and geogrid reinforced soil walls," *Geotextiles and Geomembranes,* vol. 50, p. 18, 2022.

[13] S. Vibha, " Performance of Geosynthetic Reinforced MSE Walls with Marginal Backfills at the Onset of Rainfall Infiltration," *Geosynthetics and Ground Engineering,* p. 16, 2021.

[14] H. Rahardjo, "Analyses and design of steep slope with GeoBarrier system (GBS) under heavy rainfall," *Geotextiles and Geomembranes,* vol. 48, p. 13, 2020.

[15] B. V. S. V. D. Bhattacherjee, " Numerical studies on the performance of hybrid-geosynthetic-reinforced soil slopes subjected to rainfall," *Geosynthetics International,* vol. 22, p. 17, 2015.

[16] M. Yazdandoust, "Laboratory evaluation of dynamic behavior of steel-strip mechanically stabilized earth walls," *soils and Foundations ,* 2018.

[17] S. C. Shilpa S. Vadavadagi, "Effect of rail axle load on geosynthetic reinforced back-to-back mechanically stabilized earth walls: Experimental and numerical studies," *Transportation Geotechnics ,* 2023.

[18] A. A. Samee, "Performance of back-to-back MSE walls reinforced with steel strips under seismic conditions," *Transportation Geotechnics ,* 2021.

[19] F. Ren, "Numerical study on seismic performance of tiered reinforced soil," *Soil Dynamics and Earthquake Engineering,* 2024.

[20] M. A. M. U. A. Z. B. M. O. G. T. A. A. Y. Pan Huali, "Seismic resilience of geogrid reinforced concrete earth-retaining wall of," *Structures,* p. 20, 2025.

[21] F. F. E. M. M. T. P. P. Capilleri, "Static and dynamic analysis of two mechanically stabilized earth walls," *Geosynthetics International,* 2019.

[22] Mao Yue, "Dynamic response characteristics of shaking table model tests on the gabion reinforced retaining wall slope under seismic action," *Geotextiles and Geomembranes ,* 2024.

[23] B. N. M. R. M Rama Krishna, "EVALUATION OF CBR USING GEOSYNTHETICS IN

SOIL LAYERS," *IJRET,* p. 5, 2015.

[24] Cheng Fan, "Centrifuge shaking table tests on tiered reinforced soil retaining walls subjected to the excitations of near-field ground motions," *Geotextiles and Geomembranes ,* 2024.

[25] B. Cai, "Experimental study of shaking table for reinforced soil retaining walls: Analysis of tiered configuration effects," *Soil Dynamics and Earthquake Engineering,* 2025.

[26] F. Z. ,. S. S. Bin Ge, "Seismic analysis of geosynthetic-reinforced soil walls in tiered configuration," *Geotextiles and Geomembranes,* 2024.

[27] B. M. Azmach Lole Gebeyehu, "Recent design practice of reinforced earth walls for high-speed rail transportation: A state-of-the-art and way forward," *Engineering Science and Technology,,* 2024.

[28] A. M. Amir Mohsen Safaee, "Experimental investigation on the performance of multi-tiered geogrid mechanically stabilized earth (MSE) walls with wrap-around facing subjected to earthquake loading," *Geotextiles and Geomembranes,* 2021.

[29] Ali Komak Panah, "Shaking table tests on polymeric-strip reinforced-soil walls adjacent to a rock slope," *Geotextiles and Geomembranes ,* 2021.

[30] M. G. M. R. L. A. Mirzaalimohammadia, "Pullout response of strengthened geosynthetic interacting with fine sand," *Geotextiles and Geomembranes,* p. 12, 2019.

[31] M. M. A. Johari, "System reliability analysis of geogrid reinforced retaining wall using random finite element method," *Transportation Geotechnics,* 2024.